GEOCHRONOLOGY AND GEOCHEMISTRY DATA RELEASE FOR THE NEW YORK MOUNTAINS EARTH MRI PROJECT, SAN BERNARDINO COUNTY, CALIFORNIA

U-Pb Radiometric Dating, Luminescence Dating, Geochemistry

DATA RELEASE 2026-01

Version 1.0

Compiled by

Brian J. Swanson, David Reioux, Benjamin M. Parrish, and Matthew J. Towne

Laboratory Analysis and Age Interpretation by

Joshua J. Schwartz, California State University, Northridge Laser Ablation Laboratory (U-Pb dating)

Shannon A. Mahan, U.S. Geological Survey, Luminescence Geochronology Laboratory (IRSL dating)

2026

Suggested citation:
Swanson, B.J., Reioux, D., Parrish, B.M., Towne, M.J., Schwartz, J.J., and Mahan, S.A., 2026, Geochronology and geochemistry data release for the New York Mountains Earth MRI project, San Bernardino County, California: U-Pb radiometric dating, luminescence dating, geochemistry: California Geological Survey Data Release, DR 2026-1, 18 p., Appendices A, B, and C, Supplemental Geochronology and Geochemistry Data.

STATE OF CALIFORNIA
GAVIN NEWSOM, GOVERNOR

NATURAL RESOURCES AGENCY
WADE CROWFOOT, SECRETARY

DEPARTMENT OF CONSERVATION
JENNIFER LUCCHESI, DIRECTOR

CALIFORNIA GEOLOGICAL SURVEY
JEREMY LANCASTER, STATE GEOLOGIST

Publications are available for free download from the California Geological Survey website (https://www.conservation.ca.gov/cgs).

Web Accessibility Statement - If you find any part of this document to be inaccessible with assistive technology, visit our Accessibility web page at conservation.ca.gov to report the issue and request alternative means of access. To help us respond to your concern, please include the following three items in your request: 1. your contact information. 2. the title of this document. 3. the web address where you obtained the document.

CONTENTS

SUPPLEMENTAL DATA

FIGURES

TABLES

GLOSSARY OF TERMS, ACRONYMS, AND ABBREVIATIONS

2SE analytical uncertainty – A range of values within two standard deviations (2 sigma) from the average (mean) in a normal distribution encompassing about 95% of all outcomes. Useful for internal comparison of results obtained from the same U-Pb geochronology laboratory.

AGAT Laboratories – USGS-certified contract laboratory performing geochemical analyses.

Ar – Argon.

AU – See *2SE analytical uncertainty*.

CAM – Central Age Model, used as an Equivalent Dose Model in luminescence dating.

CGS – California Geological Survey.

C1 chondrite – Reference chondritic composition used for normalized REE plots.

CSUN – California State University, Northridge.

CW-OSL (dose rate) – Continuous wave optically stimulated luminescence dose rate. The total radiation dose per unit time that the sample was exposed to during the burial period, usually expressed as radiation dose per thousand years (Gy/ka).

Dose rate – The laboratory estimate of the radiation dose accumulated throughout the burial period, expressed in SI units of gray (Gy).

EarthMRI – Earth Mapping Resources Initiative.

EBSD – Electron backscatter diffraction.

EDM – Equivalent Dose Model for luminescence dating.

Element2 SF-ICP-MS – Sector field inductively coupled plasma mass spectrometer used for U-Pb analysis.

Fe – Iron.

Ga – Giga-annum, one billion (10^9) years. Informal SI notation, where "annum" is age in years before present, with "present" fixed as 1950.

Gamma spectrometry – Technique for determining radioisotope concentrations for luminescence dose rates.

Geochemical analyses – Laboratory analyses conducted to identify and quantify the chemical (elemental and major oxide) composition or geologic materials.

GPS – Global Positioning System (context: sample location accuracy).

Gy – Gray, SI unit of absorbed radiation dose.

Gy/ka – Gray per thousand years; unit of luminescence dose rate.

He – Helium.

HREE – Heavy REE. A group of uncommon higher atomic weight rare earth elements of the lanthanide series, including dysprosium, terbium, holmium, erbium, thulium, ytterbium, lutetium, gadolinium, and yttrium, which play a significant role in high-tech applications such as permanent magnets, lasers and fiber optics.

ICP-OES-MS – Inductively coupled plasma-optical emission spectroscopy-mass spectroscopy.

ICP-MS – Inductively coupled plasma mass spectrometry.

ICP-60 – Sodium peroxide fusion method for ICP OES/MS analysis of 60 elements.

IRSL – Infrared stimulated luminescence, a burial dating technique that measures luminescence released from K-feldspar sediment grains by exposure to infrared wavelengths in order to estimate the time elapsed since a sedimentary deposit was last exposed to the sun. The method measures the buildup of luminescence in fine sand and silt grains over time due to exposure to ionizing radiation originating from the surrounding sediment as well as cosmic rays.

IsoplotR – Software package used to plot U-Pb isotopic data.

IUGS – International Union of Geological Sciences.

ka – Kilo-annum, one thousand (10^3) years. Informal SI notation, where "annum" is age in years before present, with "present" fixed as 1950.

LED – Light emitting diode.

Light REE – A group of lower atomic weight rare earth elements of the lanthanide series such as lanthanum, cerium, praseodymium, neodymium, promethium, samarium and europium, which play significant roles in various technologies such as catalysts, glass manufacturing, and magnets.

LOD – Lower limit of detection.

LOI – Loss on ignition.

Luminescence dose rate – The total radiation dose per unit time that the sample was exposed to during the burial period, usually expressed as radiation dose per thousand years (Gy/ka).

Ma – Mega-annum, one million (10^6) years. Informal SI notation, where annum is age in years before present, with "present" fixed as 1950.

Mesh – Grain size sieve designation (e.g., 80, 120 mesh).

MiniCL – Cathodoluminescence detector used for zircon imaging.

MSWD – mean square weighted deviation, a statistic describing scatter in U-Pb datasets.

NIST 612 – International glass standard used to tune ICP MS.

OSL – Optically stimulated luminescence.

pIRSL – Post-infrared infrared stimulated luminescence.

PVC – Polyvinyl chloride (tube used for luminescence sampling).

QAP diagram – Upper half of QAPF IUGS classification diagram for igneous rocks, excluding the feldspathoid-bearing rocks.

REE – Rare earth elements.

RSD – Relative standard deviation.

SAR – Single aliquot regenerative protocol for luminescence dating.

SEM – Scanning electron microscope.

Sf- ICPMS – Sector field inductively coupled plasma mass spectrometer.

T.A.S. – Total alkali silica classification diagram (Middlemost, 1994).

Total uncertainty – Total propagated uncertainty (analytical + systematic) representing a range of values incorporating the 2SE internal analytical uncertainty and a 2% systematic uncertainty that are propagated into the total uncertainty as the square root of the sum of the squared internal and systematic uncertainties to reflect the long-term accuracy of the secondary reference materials. Useful for external comparison with results from other U-Pb geochronology laboratories.

TU – See *Total uncertainty.*

U-Pb radiometric dating – Calculation of an age in years for geologic material based on the known radioactive decay rate of uranium-238 to lead-206 and uranium-235 to lead-207.

USGS – U. S. Geological Survey.

WDXRF – Wavelength dispersive x-ray fluorescence spectrometry.

WGS84 – World Geodetic System 1984 coordinate system.

XRF – X-ray fluorescence.

Geochronology and Geochemistry Data Release for the New York Mountains Earth MRI Project, San Bernardino County, California

U-Pb Radiometric Dating, Luminescence Dating, Geochemistry

Compiled by Brian J. Swanson, David Reioux, Benjamin M. Parrish, and Matthew J. Towne
Geochronology by Joshua J. Schwartz and Shannon A. Mahan

INTRODUCTION

The Mineral Resources Program at the California Geological Survey (CGS) conducted mapping within four 7.5-minute quadrangles in the New York Mountains with funding from the United States Geological Survey (USGS) Earth Mapping Resources Initiative (EarthMRI) (Grant G19AC00304). Geologic maps were completed for the Pinto Valley, Ivanpah and Castle Peaks 7.5-minute Quadrangles and the Crescent Peak Quadrangle, excluding areas within Nevada (Reioux and others, 2022a; 2022b; 2022c; 2022d). During this project, samples from selected crystalline basement rock units at twelve sites within the project area, and at type localities in immediately adjacent portions of Nevada, were collected for U-Pb radiometric dating to better define age of formation and to constrain the timing of metamorphism and deformation. The U-Pb dating was conducted by Dr. Joshua Schwartz at the California State University, Northridge (CSUN) Laser Ablation Laboratory. Radiometric dates were obtained on zircons for each sample site and titanites were dated at three of the sample sites. In addition, geochemical analyses were completed on all but one of these samples by the USGS Analytical Chemistry Project certified contract laboratory (AGAT Laboratories) and/or through the CSUN Laser Ablation Laboratory. In addition, two sediment samples were collected from older alluvial fan deposits mapped on either side of the New York Mountains to assess the age of fan deposition. Shannon Mahan at the USGS Luminescence Geochronology Laboratory conducted infrared stimulated luminescence (IRSL) dating of feldspar grains in these sediment samples. The results of all these analyses are presented in this data release.

PROJECT DESCRIPTION

The New York Mountains are a northeast-trending mountain range spanning the border of California and Nevada in northeast San Bernardino, CA, and southwest Clark, NV, Counties. Geologically the mountain range is located within the Mojave Desert geomorphic province. The eastern Mojave terrane represents the western margin of the North American craton and is underlain by Precambrian crystalline basement rocks. The Mountain Pass mine, located approximately 20 miles northwest of the study area, is the primary producer of rare earth elements (REE) in the United States. It produces light REEs that occur in bastnaesite ($CeCO_3$), which is hosted within a 1,375 ± 5 Ma carbonatite intrusive complex. The USGS identified the Mountain Pass Focus Area carbonatites and Proterozoic basement rocks as a target for future mineral exploration and development. REE mineralization and thorium anomalies have been previously identified in the New York Mountains (Miller and others, 1986).

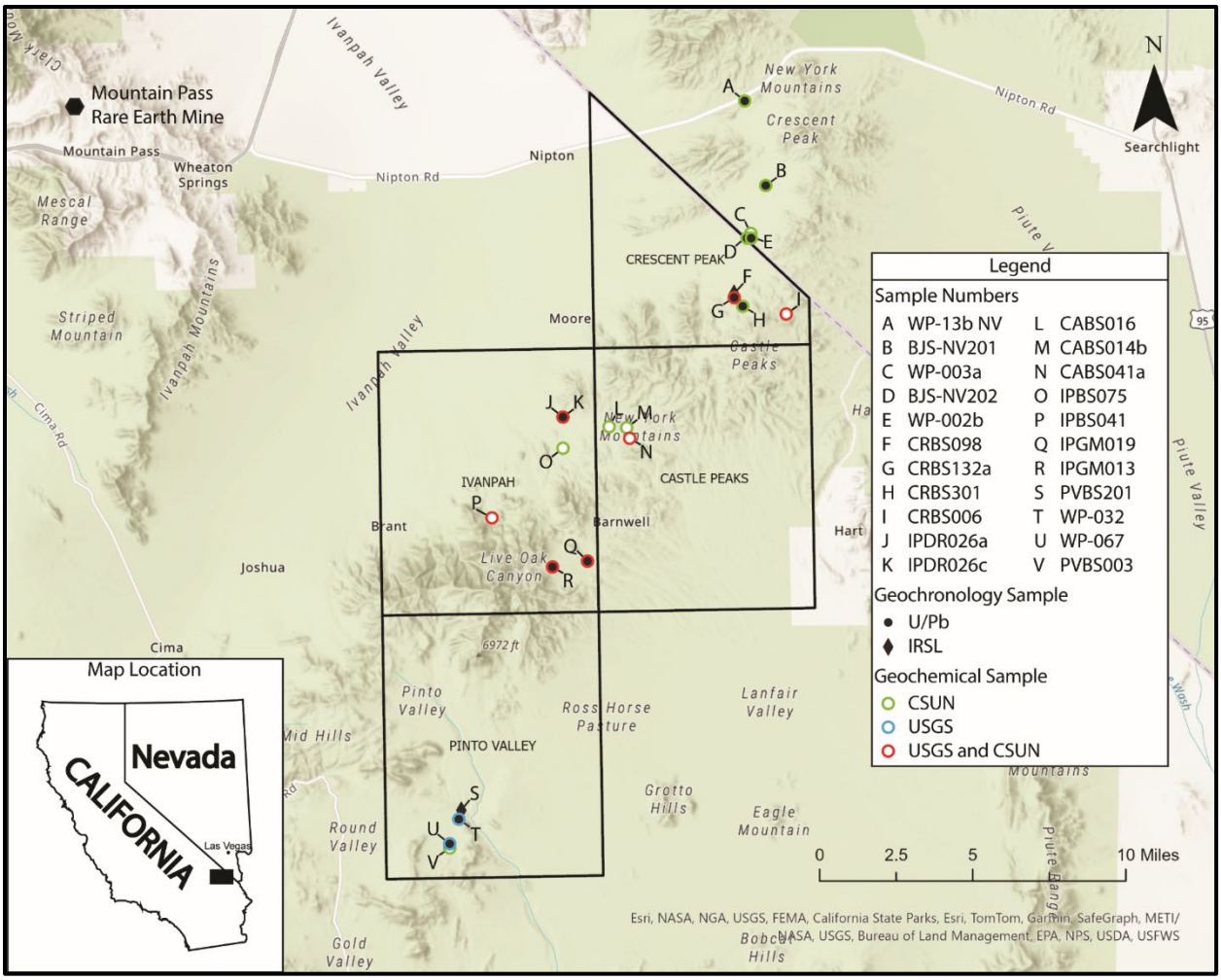

Figure 1. Location map of geochronologic and geochemical samples. The map shows both geochronologic and geochemical samples relative to the topographic quadrangles (black outlines). The project area is in eastern San Bernardino County, adjacent to the California-Nevada border.

The heavy REE mineralization has been reported to be hosted within mineralized shear zones and allanite pegmatites and dikes in the northern portion of the range near the California-Nevada border (Burns, 2011).

During the winters of 2019 to 2021, the California Geological Survey conducted 1:24,000-scale geologic mapping of the Castle Peaks, Crescent Peak, Ivanpah, and Pinto Valley 7.5-minute Quadrangles along the New York Mountains in California (Figure 1). Sample location maps are provided in Appendix A. The new geologic mapping was compiled with existing smaller-scale geologic mapping to create four preliminary 1:24,000-scale geologic maps. The final products include a single, seamless geologic data model and accompanying geologic maps for each of the four quadrangles. Funding for this project was partially provided by the USGS EarthMRI (Grant G19AC00304) and the remainder provided by the California Geological Survey.

DATING METHODOLOGIES

Sampling and Location Accuracy

Samples were collected by CGS staff during field work in 2019 and 2021. Sample locations were recorded using GPS-enabled phones or tablets using the Esri Collector application, using the World Geodetic System 1984 (WGS84) geographic coordinate system. The application recorded the accuracy of each point and sites generally within 5 m spatial uncertainty. Samples for U-Pb dating were generally 2.5 to 5 kg obtained from naturally fractured outcrops or road cuts, with a goal of acquiring relatively unweathered samples for analysis. Thin sections were prepared for each sample and representative material from all dated samples except one was also separated for geochemical analysis. Smaller surface samples were collected for geochemical analysis to support rock classification and assess potential economic mineral content. Samples were reviewed and trimmed to remove weathered rock or alteration mineralization, unless the mineralization was targeted for analysis. Documented samples were shipped either to the CSUN Laser Ablation Laboratory in Los Angeles, California, for processing and U-Pb dating and geochemical analyses, and/or to the USGS Analytical Chemistry Project Sample Control in Denver, Colorado for geochemical analysis.

Samples for luminescence dating were collected from a natural channel bank and a road cut by driving an 8-inch (20 cm)-long, 2.5-inch (6.3 cm)-diameter black PVC tube horizontally into the alluvial deposit, being careful to prevent any light contamination to the sample material. A couple kilograms of sediment were also collected from the material surrounding the tube for use in evaluating the dose rate of this material. Sand deposits exhibiting sedimentary layering were targeted for sampling as the associated depositional environment should maximize potential exposure of the sediment to sunlight at the time of deposition to record the time of burial. The samples were documented and then shipped to the USGS Luminescence Geochronology Laboratory in Denver, Colorado.

Sample Processing

CSUN Laser Ablation Laboratory

For U-Pb dating, **z**ircons were separated following standard methods involving crushing, pulverizing with jaw crusher and disk mill, and density separation on a Wilfley gold table and with heavy liquids. Samples were processed through a Frantz isodynamic separator (side tilt = 5°, front tilt = 20°) at 1.5 amps to remove magnetic (non-zircon) minerals. Zircons were poured onto double sided tape and mounted in epoxy, ground and polished. They were then imaged on a Gatan MiniCL detector attached to a FEI Quanta 600 SEM at California State University, Northridge.

USGS Luminescence Geochronology Laboratory

To determine the equivalent dose for luminescence dating, at least 5 cm of sediment was removed from both ends of the luminescence sampling tube under “safe light” (sodium vapor lighting) conditions in the luminescence laboratory. The ends and the middle portion of the samples were dried in an oven at 30° C. The dry ends were added to the bulk sediment and were crushed, homogenized and used to determine radioisotope concentrations for the dose rate.

The middle part of the sample was sieved to collect both fine (< 90 micron) and coarse-grained fraction (with fractions between 90-250 micron). The entire sample was leached in 4N HCl (10% HCl) for 24 hours, 30% H_2O_2 for 24 hours, and then sieved for 80 mesh, 100 mesh, 120 mesh, and 170 mesh sized grains. The coarser grained size (250-90 micron) quartz fractions were separated from the feldspars

and any heavy minerals using a Franz magnetic separator (for samples with a large mica or dark mineral concentrations) and heavy liquids (lithium sodium polytungstate or LST) (density = 2.58 g/cm^3 and (density = 2.67 g/cm^3). Quartz separates were not used due to concern about age underestimates and undesirable luminescence characteristics as noted elsewhere in the Mojave Desert sediments (Lawson and others, 2012). Stainless steel target discs were sprayed with silica spray and a single grain thick layer of feldspar grains was dispersed onto steel discs at a 1 to 2 mm mask.

Laboratory Analyses

CSUN Laser Ablation Laboratory

For U-Pb dating, Uranium-lead ratios were collected using a ThermoScientific Element2 SF-ICPMS coupled with a Teledyne Cetec Analyte G2 Excimer Laser (operating at a wavelength of 193 nm). Prior to analysis the Element2 was tuned using the NIST 612 glass standard to optimize signal intensity and stability. Laser beam diameter was ~25 microns at 10 Hz and 75-100% power. Ablation was performed in a HelEx II Active 2-Volume Cell™ and sample aerosol was transported with He carrier gas through Teflon-lined tubing, where it was mixed with Ar gas before introduction to the plasma torch. Flow rates for Ar and He gases were as follows: Ar cooling gas (16.0 NL/min), Ar auxiliary gas (1.0 NL/min), He carrier gas (approximately 0.3-0.5 NL/min), Ar sample gas (1.1-1.3 NL/min). Isotope data were collected in E-scan mode with magnet set at mass 202, and RF Power at 1245 W. Isotopes measured include ^{202}Hg, ^{204}(Pb+Hg), ^{206}Pb, ^{207}Pb, ^{208}Pb, ^{232}Th, and ^{238}U. All isotopes were collected in counting mode with the exception of ^{232}Th and ^{238}U which were collected in analogue mode. Analyses were conducted in a ~40-minute time resolved analysis mode. Each zircon analysis consisted of a 20-second integration with the laser firing on sample, and a 20 second delay to purge the previous sample and move to the next sample. Approximate depth of the ablation pit was ~20-30 microns.

The primary standard, 91500, was analyzed every 10-15 analyses to correct for in-run fractionation of Pb/U and Pb isotopes. A second zircon standard, Temora-2 was analyzed every ~10 analyses to assess reproducibility of the data. Total uncertainties (analytical + systematic) were determined by propagating 2% systematic uncertainties together with analytical uncertainties to reflect the long-term accuracy of the secondary reference materials. Uncertainty on the final weighted mean ages are reported in Table 2 and the Appendix B text and are first shown with analytical uncertainty followed by propagated uncertainty in brackets. U-Pb analysis of Temora-2 during all analytical sessions yielded concordant results and error-weighted average ages of 411 ± 0.4 Ma (n=280) (as reported in Schwartz and others, 2023), which is within 1.4 to 1.8% uncertainty of the accepted ages of 416.8-418.4 Ma (Black and others, 2004; Mattinson, 2010).

U-Pb isotopic data were plotted using IsoplotR (Vermeesch, 2018). Corrections for minor amounts common Pb in zircon were made following methods of Tera and Wasserburg (1972) using measured ^{207}Pb/^{206}Pb and ^{238}U/^{206}Pb ratios and an age-appropriate Pb isotopic composition of Stacey and Kramers (1975). Zircons with large common Pb corrections (e.g., analyses interpreted as having approximately 20% or greater contribution from common Pb) were discarded from further consideration. Zircon dates are reported using the ^{206}Pb/^{238}U date for zircons <1300 Ma, and the ^{207}Pb/^{206}Pb date for zircons >1300 Ma.

USGS Luminescence Geochronology Laboratory

To determine the equivalent dose for luminescence dating, post-infrared infrared luminescence measurement (pIRSL, using infra-red stimulation of potassium-feldspars) was done on a fine sand

fraction (250-180 μm) after density separation between quartz and potassium feldspar. The fine sand sized grains of potassium feldspar were measured according to parameters in Table 1 below using continuous wave and the single aliquot regenerative (SAR) protocol (Wintle and Murray, 2006). Anomalous fading tests on the stability of the luminescence signal indicated little to no signal instability. Growth curve data was fit to an exponential trend. The sample size was for multi-aliquot which means the number of grains on the disc was anywhere between 100 and 500 grains.

Table 1. Single aliquot regeneration protocol for optical dating using the CW-OSL post-IR IRSL signal from K-feldspar (from Kars and others, 2014).

1.	Preheat (230° C) for 60 seconds (s)
2a.	IRSL stimulation with infrared LED (870 nm) at 100° C for 100 s (L_n) (not used)
2b.	IRSL stimulation with infrared LED (870 nm) at 230° C for 100 s (L_n) (post-IR IRSL)
3.	Test dose beta irradiation
4.	Preheat (230° C) for 60 s
5a.	IRSL stimulation with infrared LED (870 nm) at 100° C for 100 s (T_n) (not used)
5b.	IRSL stimulation with infrared LED (870 nm) at 230° C for 100 s (T_n) (post-IR IRSL)
6.	Beta irradiation of regeneration dose
7.	Preheat (230° C) for 60 s
8a.	IRSL stimulation with infrared LED (870 nm) at 100° C for 100 s (L_x) (not used)
8b.	IRSL stimulation with infrared LED (870 nm) at 230° C for 100 s (L_x) (post-IR IRSL)
9.	Test dose beta irradiation
10.	Preheat (230° C) for 60 s
11a.	IRSL stimulation with infrared LED (870 nm) at 100° C for 100 s (T_x) (not used)
11b.	IRSL stimulation with infrared LED (870 nm) at 230° C for 100 s (T_x) (post-IR IRSL)
12.	Repeat steps 6-11 with further regeneration doses with one of the steps a “zero” dose

For purposes of determining the dose rate for luminescence dating, it is recognized that most ionizing radiation in the sediment is from the decay of isotopes in the uranium and thorium decay chains and the radioactive potassium-40 element. The dose rate was obtained by both gamma spectrometry and ICP-MS analyses. The ICP-MS analyses are described in the geochemistry section below. The concentrations of K, U, Th, and Rb were determined using gamma spectrometry following the procedures described in Snyder and Duvall (2003). The gamma-ray spectrometer provides the isotopic discrimination of gamma rays; correspondingly, beta and alpha dose rates may be estimated. In the laboratory, the bulk samples were counted in a low-resolution gamma spectrometer fitted with a germanium detector. Measured elemental concentrations, associated dose rates, and cosmic ray contributions are presented in tables. Cosmic-ray dose rate data was estimated for each sample as a function of depth, elevation above sea level, and geomagnetic latitude (Prescott and Hutton, 1994).

Sampling sub-sets (multiple small samples around a luminescence sample site) were compared against each other to detect any inhomogeneous geologic conditions (i.e. large stones, clay layers, or cementation) and to fully account for any gamma activity that the luminescence sample received from

layers above and below that might have had differing grain size or geologic source. For this purpose, the bulk samples were dried, homogenized by gentle disaggregation, weighed, sealed in plastic planchets having a diameter of 15.2 cm by 3.8 cm (some modification from Murray and others, 1987), and then immediately placed in a gamma-ray spectrometer for about 8.5 hours. Samples were then stored for a minimum of 21 days to allow radon to achieve radioactive equilibrium and the measurements were repeated. The fraction of radon emanation was estimated from the difference of these two spectrometer measurements. A sealed/unsealed ratio of <1.10 is not considered to represent significant radon escape under laboratory conditions. These count rates are accurate for calculating dose rates. Alpha and beta contributions to the dose rate were corrected for grain-size attenuation (Aitken, 1985).

GEOCHEMICAL METHODOLOGIES

CSUN Laser Ablation Laboratory

Bulk-rock samples were powdered in an alumina ceramic shatter-box. Powders were mixed with a 2:1 ratio of SpectroMelt A10 lithium tetraborate flux and melted at 1,000° C for approximately 20 minutes to create glass beads at California State University, Northridge. Beads were re-powdered, re-fused following the initial melting parameters, and polished to remove carbon from the flat bottom where analysis occurs. Following procedures outlined in Lackey et al. (2012), glass beads were analyzed at Pomona College for major (SiO_2, TiO_2, Al_2O_3, Fe_2O_3, MnO, MgO, CaO, Na_2O, K_2O, P_2O_5) and trace (Rb, Sr, Ba, Zr, Y, Nb, Cs, Sc, V, Cr, Ni, Cu, Zn, Ga, La, Ce, Pr, Nd, Hf, Pb, Th, U) elements by X-ray fluorescence (XRF). Beads were analyzed with a 3.0 kW Panalytical Axios wavelength-dispersive XRF spectrometer with PX1, GE, LiF 220, LiF 200, and PE analyzer crystals.

USGS AGAT Laboratories

To meet the USGS quality assurance/quality control (QA/QC) standards and data release requirements, geochemical analysis was performed by the USGS contract laboratory, AGAT Laboratories. Samples collected for geochemical analysis were submitted to the USGS Analytical Chemistry Project for sample preparation and submission to AGAT Laboratories. The data was then verified by the USGS using known QC samples, duplicate analyses and other QA/QC procedures that are part of the routine USGS approved process (USGS, 2021). The following methods were provided by the Analytical Chemistry Project for sample preparation and analyses:

Sample Preparation

The materials were ground in a pulverizer equipped with ceramic plates or a disc mill using an alumina corundum or agate chamber. All rock samples were ground to <200 mesh. All sediment and soil samples were ground to <150 mesh. All samples were mixed after preparation to ensure homogeneity for subsequent analysis.

WDXRF Major Element Analysis

Major elements are determined in rocks and minerals by wavelength dispersive x-ray fluorescence spectrometry (WDXRF). The sample is fused with lithium metaborate/lithium tetraborate flux and the resultant glass disk is introduced into the WDXRF and irradiated by an x-ray tube. The method also provides a gravimetric loss on ignition (LOI). Data will be deemed acceptable if recovery of the major oxides is ± 5% at the lower limit of detection (LOD) and the calculated percent relative standard deviation (RSD) of duplicate samples is no greater than 5%.

Sixty Elements by Inductively Coupled Plasma-Optical Emission Spectroscopy-Mass Spectroscopy (ICP-OES-MS), Sodium Peroxide Fusion (ICP-60)

Sixty elements are determined in rocks, minerals and soils. Samples are fused at 750°C with sodium peroxide and the fusion cake dissolved in a dilute nitric acid. The resulting solution is analyzed by ICP-OES and ICP-MS. Data will be deemed acceptable if recovery of each element is ± 15% at five times the LOD and the calculated RSD of duplicate samples is no greater than 15%.

GEOLOGIC UNIT DESCRIPTIONS

Descriptions for the geologic units sampled for U-Pb dating (12), IRSL dating (2), and for geochemical analyses (28) are provided below. New geochronology data and photographic imagery for each sample is presented in Appendix B and summarized in Tables 2 and 3. Geologic unit descriptions are abridged from the descriptions provided in Reioux and others (2022a-d). Unit descriptions are supplemented by sample-specific mineral composition and textural descriptions that are based on petrographic review of thin sections. Igneous rock names were determined using an IUGS plutonic rock classification ternary diagram with normalized quartz, alkali feldspar, and plagioclase values (QAP diagram) from the petrographic review. For comparison, igneous rock names derived from geochemical analyses of the same samples based on total alkali versus silica compositions, as classified by Middlemost (1994), can be found in Figures C1 and C2 in Appendix C. Chondrite-normalized spider diagram plots of the rare earth elements are provided in Figures C3 and C4 in Appendix C.

Qof **Older fan deposits (late to middle Pleistocene)**—Slightly to moderately consolidated, poorly sorted, silty, pebbly sand to coarse gravel and boulder fan deposits. Deposits underlie broad to erosionally isolated fan surfaces at least several meters above active channel grade that are moderately dissected and support stable vegetation; not subject to historic flood inundation; clasts exhibit moderate oxidation/desert varnish patinas and desert pavement.

Sample PVBS201 (IRSL date) is a light yellowish-brown to brownish-yellow (10YR 6/4-6/6) older alluvial deposit composed of medium- to coarse-grained sand with silt that is exposed on the east flank of the New York Mountains; slightly friable; bedding is weakly developed and medium thick (10-30 cm). Sample collected in a road cut about 25 m below original fan surface, which is about 2.5 m above the adjacent channel grade of Watson Wash.

Sample CRBS098 (IRSL date) is a light yellowish-brown to very pale brown (10YR 7/4-6/6) older alluvial deposit exposed on the west flank of the New York Mountains that is a locally bedded, silty sand to gravelly sand and gravel with common caliche; locally friable. Sample collected in channel bank about 2 m below original fan surface, which is about 1 m above the adjacent channel grade.

Cretaceous Granitoid Rocks of the Teutonia Batholith (Klo, Kmh, and Krs)

Klo **Live Oak Canyon Granodiorite (Late Cretaceous)—**Light-gray to salt-and-pepper to tan biotite granodiorite that is typically medium- to coarse-grained with hypidiomorphic and equigranular texture and locally porphyritic near the Mid Hills Quartz Monzonite (Kmh) with alkali feldspar phenocrysts (Miller and Wooden, 1993). Biotite is the primary mafic mineral; other accessory minerals commonly include hornblende, opaque oxides, titanite, allanite and apatite (Beckerman, 1982). Quartz porphyry and undifferentiated dikes are common within the unit.

Sample IPGM019 (Quartz porphyry dike cutting Klo - U-Pb dating of zircons and geochemistry by both laboratories) is a white to light-gray quartz porphyry dike that weathers dark reddish brown to light orangish brown. Mineral composition is 15% medium- to coarse-grained quartz including commonly fractured subhedral phenocrysts up to 7 mm, 10% medium- to coarse-grained subhedral plagioclase, which has been heavily altered by sericite, 10% medium- to coarse-grained subhedral potassium feldspar which has been heavily altered, 5% medium-grained tabular muscovite, 2% fine-grained biotite, and 58% microcrystalline groundmass with a salt-and-pepper appearance.

Sample IPGM013 (Klo - U-Pb dating of zircons and geochemistry by both laboratories) is a salt-and-pepper colored monzogranite. In hand sample, medium- to coarse-grained, hypidiomorphic, equigranular minerals are cut by a medium-grained dike with similar minerology. Petrographic observations revealed a mineral composition of 35% medium- to coarse-grained subhedral plagioclase with common zoning and minor sericite alteration, 32% medium- to coarse-grained subhedral mosaic quartz, which displays undulose extinction, 25% coarse-grained subhedral potassium feldspar displaying tartan twinning, which is locally destroyed by alteration, and 5% medium- to coarse-grained tabular biotite. Accessory minerals include 3% opaque oxides that are associated with biotite, and trace titanite. Approximately 25% of the thin section is the medium-grained dike. Compared to the rest of the slide, this area has a slight (<5%) increase in quartz and equal decrease in feldspars.

Kmh **Mid Hills Quartz Monzonite (Late Cretaceous)—**Salt-and-pepper to light-gray to tan, medium- to coarse-grained granite to quartz monzonite with porphyritic to equigranular texture Cretaceous composed primarily of alkali feldspar, plagioclase and quartz with secondary biotite and hornblende; typical accessory minerals include opaque oxides, titanite (sphene), allanite and apatite (Beckerman, 1982); adamellite of Beckerman (1982) and Miller and Wooden (1993); the porphyritic phase contains euhedral to subhedral alkali feldspar phenocrysts. Commonly cut by aplite and pegmatite dikes (Miller and Wooden, 1993). Contains local foliated hornblende granodiorite enclaves, one of which was dated in this study as late Early Cretaceous (WP-067).

Sample IPBS041 (Kmh – Geochemistry by both laboratories) is a salt-and-pepper colored porphyritic granite. Mineral composition is 40% medium-grained quartz, 38% coarse-grained plagioclase, 17% coarse-grained potassium feldspar, and 5% medium-grained biotite. Euhedral tabular to equant potassium feldspar phenocrysts up to 3 cm in maximum dimension are common.

Sample PVBS003 (Kmh – Geochemistry by CSUN) is a brownish-gray foliated granite dike. The mineral composition is 50% medium-grained quartz with quartz rods common, 25% medium-grained plagioclase, 22% medium-grained potassium feldspar, 3% fine-grained elongate biotite with some chloritization, 1% secondary muscovite with some chloritization, and 1% opaques. The foliation is parallel to dike trend and is expressed in all minerals with the elongation in the direction of foliation.

Sample WP-067 (PVBS005) and PVDR03 (hornblende granodiorite enclave in Kmh - U-Pb dating of zircons and titanites (WP-067 (PVBS005)) and geochemistry by USGS (PVDR03)) is an enclave within the Kmh that is composed of foliated salt-and-pepper colored hornblende

granodiorite that weathers to dark gray. This sample is from one of the many mafic inclusions in the Mid Hills Quartz Monzonite. At outcrop scale, this sample is equigranular, foliated, and appears much darker than most of the Mid Hills Quartz Monzonite. The sample has a mineral composition of 28% fine- to medium-grained subhedral plagioclase with varying amounts of fracturing and sericitic alteration, 24% fine- to medium-grained anhedral quartz with sutured boundaries, 20% medium-grained anhedral hornblende associated with biotite, 15% subhedral biotite, 10% fine- to medium-grained anhedral potassium feldspar with little to no twinning, and 3% disarticulated titanite. Aligned hornblende and biotite grains define the foliation.

Krs **Rock Springs Monzodiorite (Late Cretaceous)—**Salt-and-pepper to gray, medium-grained diorite to granodiorite composed of plagioclase and lesser amounts of alkali feldspar, quartz, biotite, and hornblende with abundant, elongate biotite and hornblende mafic inclusions oriented along weak to moderate foliation; cut by common aplite dikes (Beckerman, 1982).

Sample WP-032 (PVBS001a) and PVDR001 (Krs - U-Pb dating of zircons and titanites (WP-032 (PVBS001a)) and geochemistry by USGS (PVDR001)) is a salt-and-pepper colored quartz monzodiorite that weathers to pink. At outcrop scale, variably developed foliation is expressed by mafic minerals. Petrographic analysis shows mineral composition of 45% coarse-grained subhedral plagioclase that displays both zoned and more abundantly albite twinning textures, 22% coarse-grained subhedral potassium feldspar, 15% fine- to medium-grained anhedral quartz with sutured boundaries common, 10% medium-grained subhedral biotite, 5% medium-grained subhedral hornblende, and 3% iron oxides. Myrmekite texture in plagioclase is observed at 1% of the boundaries between quartz and plagioclase. In thin section a weak foliation is defined by aligned biotite and hornblende grains.

Mzv **Volcanic and sedimentary rocks (Mesozoic)**—Metamorphosed rhyolites and sedimentary rocks (Miller and Wooden, 1993) including vitric rhyolitic tuffs, lithic rhyolitic tuffs, and quartzites.

Sample IPBS075 (MZV-2) (Mzv – Geochemistry by CSUN) is a gray fine-grained metavolcanic rock. The mineral composition is 80% very fine- to fine-grained quartz groundmass and local fine-grained quartz veins, 15% medium-grained heavily altered feldspar, 3% very fine-grained biotite, and 2% opaques. Alteration has obscured/destroyed most feldspar twinning; Carlsbad and albite twinning are preserved rarely and show two populations of feldspars.

Xbg **Biotite-garnet gneiss of Willow Wash (Paleoproterozoic)**—Gray to brown weathering, well-foliated gneisses consisting of intermixed biotite garnet gneiss, quartzo-feldspathic gneiss, biotite-sillimanite gneiss, local fine-grained augen gneiss similar to unit Xfp, and migmatite. The unit also includes locally common deformed pegmatite bodies and 1- to 2-m-wide, foliation-parallel, medium-grained phaneritic to porphyritic, quartzo-feldspathic dikes or leucosomes, with and without garnet. The unit becomes increasingly mylonitic to the east with augen-shaped feldspar porphyroclasts and an augen-gneissic texture (Miller and Wooden (1994).

Sample IPDR026a (Xbg - U-Pb dating and geochemistry by both laboratories) is a black-and-white garnet-kyanite-biotite gneiss that weathers to brown and white. This sample has a mineral composition of 40% medium- to coarse-grained anhedral quartz with undulose extinction, 15% medium- to coarse-grained anhedral potassium feldspar with microcline twinning and dissolution crinkle textures, 1% medium-grained anhedral plagioclase, 15% fine- to medium-grained tabular biotite, 3% fine-grained blocky aluminosilicate (kyanite?), 1% disarticulated garnet with quartz intergrowths, 2% opaques, and 23% secondary chlorite that is pervasive and has altered the majority of the plagioclase and rimmed the kyanite. Metamorphic foliation is defined by aligned tabular biotite grains and by segregated leucocratic bands of quartz and feldspar.

Sample IPDR026c (Xbg (similar to Xfp) - U-Pb dating and geochemistry by both laboratories) is a dark greenish-gray mylonitic augen gneiss with a fine-grained matrix, similar in composition to unit Xfp mapped elsewhere. IPDR026c has a mineral composition of 50% fine- to coarse-grained tabular biotite, 22% medium-grained anhedral to subhedral quartz with sutured boundaries forming ribbons in the direction of foliation, 15% medium- to very coarse-grained anhedral to subhedral plagioclase with moderate sericitic alteration, 5% fine- to medium-grained subhedral potassium feldspar, 5% coarse-grained subhedral garnet with fractures filled by biotite, 3% rutile, and trace ilmenite associate with rutile. Mylonitic foliation is defined by quartz ribbons and aligned biotite grains; augens are composed of plagioclase grains, up to 1 cm.

Sample CABS014b (Xbg – Geochemistry by CSUN) is a dark greenish-brown biotite augen gneiss. Approximate mineral composition is 50% quartz, 40% feldspar, and 10% biotite. Quartz bands are commonly observed bending around pink to off-white potassium feldspar augen up to 3 cm in length. Locally larger deformed pink potassium feldspar forms small boudins up to 8 cm in length and some larger pegmatitic seams.

Sample CABS016 (Xbg – Geochemistry by CSUN) – is a white to gray migmatite with white contorted/variably felsic bands in a light-gray gneissic matrix. The mineral composition is 40% fine- to medium-grained plagioclase, 30% fine- to coarse-grained quartz with undulatory extinction common,15% medium-grained garnet that is highly fractured with some biotite-filled fractures, 10% fine- to medium-grained biotite, 4% secondary sericite, and 1% opaques that are associated with the biotite and garnet. Biotite grain alignment defines metamorphic foliation with locally ptygmatic folding.

Sample CABS041a (Xbg – Geochemistry by both laboratories) is a pale pink to pale orange mylonitic pegmatite. The mineral composition consists of 51% very fine-grained pale pink to pale orange matrix of primarily potassium feldspar and plagioclase with 30% medium grained clear to white quartz forming elongate ribbons. Quartz ribbons are commonly a few millimeters wide by a few centimeters long, however in the more pegmatitic areas the quartz resembles a continuous vein that is a few centimeters wide. The quartz ribbons are commonly bent around larger feldspars that are slightly darker than the matrix. The larger feldspar grains are composed of 15% medium grained potassium feldspar and 3% medium grained plagioclase. 1% opaques are associated with medium grained quartz and feldspar. A lighter reaction rim is observed between many of the medium grained quartz and feldspar clasts. The foliation is defined by the quartz ribbons.

Xlg **Leucocratic granite (Paleoproterozoic)—**Metamorphosed, subequigranular, light-brown to white weathering leucocratic granite with accessory biotite, and local accessory garnet. Unfoliated to weakly foliated, with localized zones of mylonitic fabric but also cuts older mylonites.

Sample CRBS301 (Xlg - U-Pb dating of zircons and geochemistry by CSUN) is a pinkish-orange meta-leucocratic monzogranite that weathers to light brown. The sample has a mineral composition of 33% coarse-grained subhedral to anhedral potassium feldspar with local fracturing and plagioclase inclusions, 31% medium- to coarse-grained anhedral quartz with sutured boundaries and occurring both in ribbons bending around coarse-grained feldspar grains and in mats, 27% coarse-grained subhedral plagioclase with moderate to extensive sericitic alteration, 5% anomalous blue and yellow secondary chlorite replacing biotite, 3% rutile associated with sericite locally present within heavily altered medium-grained plagioclase, and 1% medium-grained subhedral muscovite.

Xlgf **Leucocratic fine-grained to porphyritic rock (Paleoproterozoic)—**Local facies of Xlg consisting of resistant, light greenish-gray to yellowish-gray weathering fine-grained silicic rock with local weakly deformed euhedral to anhedral feldspar phenocrysts less than 1 cm in maximum dimension; the texture and grain size suggest this unit had a silicic volcanic protolith.

Sample CRBS132a (Xlgf - U-Pb dating and geochemistry by both laboratories) is a green to greenish-gray altered metavolcanic rock. Mineral composition is 40% secondary sericite replacing plagioclase and intermixed with epidote, 30% secondary epidote forming mats with the sericite, 20% medium-grained anhedral quartz with sutured boundaries, and 10% highly altered medium-grained subhedral to anhedral plagioclase.

Xbt **Granodiorite of Big Tiger Wash (Paleoproterozoic)—**Metamorphosed, variably porphyritic biotite granodiorite. Potassium feldspar phenocrysts, up to 3 cm, commonly form tabular euhedral laths, with a crude, laterally variable alignment along weak mylonitic or possibly primary foliation.

Sample WP-135b NV (Xbt - U-Pb date and geochemistry by CSUN) is a light gray syenogranite, representing the leucocratic phase of Xbt. Mineral composition is 45% tartan twinned anhedral potassium feldspar occurring as coarse-grained phenocrysts and fine- to medium-grained mats, 32% fine- to medium-grained anhedral quartz with sutured boundaries and localized ribbons, 20% coarse-grained anhedral plagioclase showing heavy sericitic alteration, excluding inclusions in potassium feldspar, and 3% medium-grained biotite locally replaced by chlorite. Uncommon (<1%) myrmekite was observed on grain boundaries between plagioclase and potassium feldspar.

Xcj **Granodiorite of Crippled Jack Well (Paleoproterozoic)—**Dark-gray to brown weathering, salt-and-pepper colored hornblende-biotite meta-granodiorite with abundant mafic minerals (up to 40%) and local accessory garnet. Dominantly porphyritic and variably mylonitic.

Sample WP-002b (Xcj - U-Pb dating of zircons and titanites and geochemistry by CSUN) is a dark-gray to salt-and-pepper colored porphyritic mylonitic biotite-monzogranite that

weathers dark gray to brown. Mineral composition is 25% medium-grained anhedral quartz ribbons with sutured boundaries and microcrystalline quartz (1-2%), 25% coarse-grained slightly altered subhedral potassium feldspar, 25% fine-grained biotite, 20% coarse-grained subhedral plagioclase with slight sericitic alteration and altered twinning, 3% ilmenite, and 2% titanite. Aligned biotite grains and quartz ribbons define local mylonitic foliation.

Sample BJS-NV201 (Xcj - U-Pb dating of zircons and geochemistry by CSUN) is a dark-gray to salt-and-pepper colored mylonitic granodiorite that weathers dark gray to brown. The sample has a mineral composition of 40% medium- to coarse-grained extensively sericite altered (up to 45%) subhedral to anhedral plagioclase, 30% fine- to medium-grained anhedral quartz ribbons with sutured boundaries and undulose extinction, 12% medium- to coarse-grained anhedral potassium feldspar, 15% secondary anomalous blue, locally bent chlorite, and 3% opaques that are parallel to veins and associated with chlorite and sericite. Quartz ribbons and chlorite define the mylonitic foliation.

Sample BJS-NV202 (Xcj - U-Pb dating of zircons and geochemistry by CSUN) is a dark-gray to salt-and-pepper colored granodiorite that weathers dark gray to brown. Mineral composition is 34% medium- to coarse-grained subhedral plagioclase extensively altered to sericite, 25% medium- to coarse-grained and microcrystalline quartz with large anhedral grains displaying undulose extinction and rimmed by recrystallized microcrystalline quartz, 20% fine- to medium-grained biotite cross-cutting plagioclase and/or locally kinked, 15% coarse-grained subhedral potassium feldspar, 5% anomalous yellow secondary chlorite found in mats and as an alteration product of biotite, and 1% opaques associated with the biotite. A weak mylonitic foliation is defined by oriented biotite, chlorite, and the coarser elongate feldspar grains.

Sample WP003a (Xcj – Geochemistry by CSUN) is a grey to brown foliated porphyritic granodiorite with stretching lineation. The sample is 70% leucocratic minerals and 30% mafic minerals. The leucocratic portion is composed of plagioclase, potassium feldspar, and quarts. White to pinkish-gray feldspar porphyroclasts up to about 5 mm in diameter form discontinuous foliated bands intermixed with gray quartz and chlorite. Biotite is the primary mafic mineral. A weak mylonitic fabric with poorly defined partings is observed at outcrop scale and is cut by epidote veins.

Xgnt **Leucocratic granite with garnet clots (Paleoproterozoic)—**Metamorphosed, light-brown weathering, subequigranular leucocratic granite with prominent glomeroporphyroblastic garnets up to 2 cm; otherwise similar to Xlg.

Sample CRBS006 (Xgnt – Geochemistry by both laboratories) – is a white to light brown garnetiferous leucogranite. Mineral composition consists of 35% coarse-grained quartz with undulatory extinction, 30% coarse-grained potassium feldspar, 25% coarse-grained plagioclase with locally extensive sericitic alteration, 7% medium-grained tabular to euhedral biotite, and 3% highly fractured garnet up to 10 mm in maximum dimension.

GEOCHRONOLOGY RESULTS SUMMARY

The results of U-Pb dating of twelve rock samples, conducted by Josh Schwartz at the CSUN Laser Ablation Laboratory, are summarized in Table 2. Luminescence dating results for two alluvial fan

samples using IRSL methods, conducted by Shannon Mahan at the USGS Luminescence Laboratory, are summarized in Table 3 and full data is provided in the USGS Data Release by Mahan and others (2026).

Sample location maps are provided in Appendix A. Appendix B presents graphical plots illustrating the basis for the reported ages, representative photographs of each rock or alluvial material analyzed, photomicrographs of associated thin sections, and descriptions of the results including comparisons to previous geochronologic studies of the subject units. Raw data for all analyses are provided as supplemental material in Excel files titled: "Schwartz Master U-Pb Geochron Table 2.11.26" for U-Pb dates and "USGS Luminescence Data_NY Mtns_FINAL" for IRSL dates, with associated data dictionary file (USGS Luminescence Data_NY Mtns_Data_Dictionary).

Table 2. Summary of results: U-Pb Dating of Zircons

Quad	Sample No.	Geologic Unit	Latitude	Longitude	Age (Ma)	AU	TU	MSWD	No. Z
IP	IPGM019**	Qtz porph. dike	35.27407	-115.25681	73.3	1.4	2.0	1.1	4/22
IP	IPGM013**	Klo	35.27167	-115.27695	69.2	0.6	1.5	3.7	21/34
PV	WP-032[1]***	Krs	35.15278	-115.33332	92.1	0.9	2.1	1.9	20/25
PV	WP-067[1]***	Enclave in Kmh	35.14133	-115.33916	107.5	0.7	2.3	2.5	27/40
IP	IPDR026a**	Xbg	35.34258	-115.26942	1,679	30	45	2.1	19/50
IP	IPDR026c**	Xfp in Xbg	35.34258	-115.26942	1,715	37	50	0.75	50/50
CR	CRBS301*	Xlg	35.39395	-115.16452	1,693	12	36	4.2	50/50
CR	CRBS132a**	Xlgf	35.39786	-115.16935	1,793	40	54	0.4	49/50
CR/NV	WP-135NVb*	Xbt	35.49082	-115.16113	1,700	6	34	1.4	36/40
CR/NV	WP-002b[1]*	Xcj	35.42622	-115.15868	1,685	7	34	0.6	35/40
CR/NV	BJS-NV201*	Xcj	35.45074	-115.14973	1,659	17	37	0.5	48/50
CR/NV	BJS-NV202*	Xcj	35.42624	-115.16074	1,707	7	35	3.4	35/37

Notes: Reported uncertainties include the 2SE Analytical Uncertainty (AU), for internal laboratory comparison, and the Total Uncertainty (TU) summed from the propagated 2% systematic uncertainty + analytical uncertainty, for external laboratory comparison; data scatter is represented by the mean square weighted deviation (MSWD). No. Z is number of zircons used to determine the age, followed by the total number of zircons analyzed. IP = Ivanpah 7.5' Quadrangle; PV = Pinto Valley 7.5' Quadrangle; CR = Crescent Peak 7.5' Quadrangle; CR/NV = Crescent Peak 7.5' Quadrangle in Nevada
*Geochemistry completed for sample through the CSUN Laboratory.
** Geochemistry completed for sample at both CSUN and USGS AGAT Laboratories.
*** Geochemistry completed for sample at the USGS AGAT Laboratory; note that sample WP-032 is same locality as PVDR001 and sample WP-067 is the same locality as PVDR003 in plots in Appendix C.
[1]Titanite U-Pb dating also completed (see Appendix B).

Table 3. Summary of Results: IRSL dating of sedimentary feldspar grains.

Quad	Sample No.	Geologic Unit	Latitude	Longitude	Age (yrs)	1SE	Range (ka)	EDM
CR	CRBS098	Qof	35.40090	-115.16900	70.1	7.3	63-77	CAM
PV	PVBS201	Qof	35.15699	-115.33196	40.7	1.4	39-42	CAM

Notes: Reported error is 1 sigma; EDM = Equivalent Dose Model; CAM = Central Age Model. Complete sample information can be found in the USGS Science Database at: https://doi.org/10.5066/P13JP7LJ.

GEOCHEMICAL RESULTS SUMMARY

Geochemical analyses were completed to document the composition of each dated rock sample, plus analyses were completed on additional selected rock samples, as noted in the geologic unit descriptions. The raw data results of geochemical analyses by both the CSUN and USGS Labs are provided as supplemental data as tabs in an Excel spreadsheet titled "Geochem_Data_Table_CSUN-USGS_Results_Combined". The CSUN WXRF results of major oxides, and 28 trace elements include data for 18 individual samples and duplicate analyses for samples IPGM013 and BJS-NV201. Eight of the samples analyzed by CSUN plus an additional two samples (PVDR-001, and PVDR-003) were also analyzed by the USGS for major oxides and 60 elements using WXRF and ICP-MS respectively (USGS, 2021).

Sample location maps are provided on Figure 1 and in Appendix A. Rock names based on total alkali versus silica composition plots (Middlemost, 1994), and Chondrite-normalized spider diagram plots (Sun and McDonough, 1989) of the rare earth elements are provided in Appendix C.

Geochemical results from the USGS analysis displayed on the C1 Chondrite-normalized Rare Earth Element (REE) spider diagrams (Sun and McDonough, 1989) in Appendix C show elevated concentrations of lanthanum from samples CRBS132a and IPDR026c, with CRBS132a having slightly less than 800 times C1 Chondrite-normalized concentrations. However, average REE concentrations for high grade samples from the Thor and Mountain Pass rare earth deposits (Bruns, 2011) are about 2 orders of magnitude more enriched than CRBS132a. Additionally REE concentrations in CRBS123a and IPDR026a decrease much more prominently towards the HREE portion of the plot than the high-grade samples from the Thor and Mountain Pass deposits.

Ideally for silica rocks the total oxide weight percents for each analysis should be between 98.5%-101.5% (Rollinson, 1993). All the USGS analysis fell within this window, however 5 analyses from CSUN area yielded greater than 101.5% total oxides. This includes both analysis of IPGM013 (108.9% and 108.8%) and both analysis of BJS-NV201 (103.1% and 105.9%). For the purposes of this report this information was included and plotted the same as all other data. However, the reader should use caution when interpreting these data.

ACKNOWLEDGEMENTS

The New York Mountains mapping project was financially supported by the USGS EarthMRI Grant No. G19AC00304 and matching funds from CGS, and the USGS conducted the analyses for the noted USGS geochemical data. The authors would like to thank Erica Key and Catherine Wesoloski who worked with the CSUN Laboratory to help run the titanite dates presented in this report. We thank Alex Lusk for providing input on the titanite dating and providing image D in Figure B10. Chris Henningfeld assisted with formatting the geochemical T.A.S. diagrams in Appendix C.

REFERENCES CITED

Aitken, M.J., 1985, Thermoluminescence dating: London, Academic Press, 359 p.

Beckerman, G.M., Robinson, J.P., and Anderson, J.L., 1982, The Teutonia batholith—A large intrusive complex of Jurassic and Cretaceous age in the eastern Mojave Desert, California, in Frost, E.G., and Martin, D.M., eds., Mesozoic-Cenozoic tectonic evolution of the Colorado River region, California, Arizona, and Nevada: San Diego, California, Cordilleran Publishers, p. 205-220.

Black, L.P., Kamo, S.L., Allen, C.M., Davis, D.W., Aleinikoff, J.N., Valley, J.W., Mundil, R., Campbell, I.H., Korsch, R.J., Williams, I.S., and Foudoulis, C., 2004, Improved Pb-206/U-218 microprobe geochronology by the monitoring of a trace-element-related matrix effect; SHRIMP, ID-TIMS, ELA-ICP-MS and oxygen isotope documentation for a series of zircon standards: Chemical Geology, v. 205, p. 115-140.

Bruns, J.J., 2011, Rare earth mineralization of southern Clark County, Nevada [Senior thesis]: California State Polytechnic University, Pomona, 38 p.

Burchfiel, B. C., and Davis, G. A., 1971, Clark Mountain thrust complex in the Cordillera of southeastern California: Geologic summary and field trip guide: California University, Riverside, Campus Miscellaneous Contribution, no. 1, p. 1-28.

Burchfiel, B.C., and Davis, G.A., 1977, Geology of the Sagamore Canyon-Slaughterhouse Spring area, New York Mountains, California: Geological Society of America Bulletin, v. 88, no. 11, p. 1,623-1,640.

Kars, R.H., Reinmann, T., and Wallinga, J., 2014, Are feldspar SAR protocols appropriate for post-IR IRSL dating?: Quaternary Geochronology, p. 126-136.

Lawson, M.J., Roder, B.J., Stang, D.M., and Rhodes, E.J., 2012, OSL and IRSL characteristics of quartz and feldspar from southern California, USA: Radiation Measurements, v. 47, p. 830-836.

Mahan, S.A., Swanson, B.J., Krolczyk, E.T., and Reioux, D., 2026, Luminescence data associated with the New York Mountains Earth Mapping Resources Initiative Project, San Bernardino County, California, 2019-2021: U.S. Geological Survey Data Release, https://doi.org/10.5066/P13JP7LJ.

Mattinson, J.M., 2010, Analysis of the relative decay constants of ^{235}U and ^{238}U by multi-step CA-TIMS measurements of closed-system natural zircon samples: Chemical Geology, v. 275, p. 186-198.

McDonough, W.F., and Sun, S.-s., 1995, The composition of the Earth: Chemical Geology, v. 120, p. 223-253.

Middlemost, E.A.K., 1994, Naming materials in the magma/igneous rock system: Earth-Science Reviews, v. 37, p. 215-224.

Miller, D.A., Frisken, J.G., and Jachens, R.C., 1986, Mineral resources of the Castle Peaks Wilderness Study Area, San Bernardino County, California: U.S. Geological Survey Bulletin 1713- A, 17 p.

Miller, D.M., and Wooden, J.L., 1993, Geologic map of the New York Mountains area, California and Nevada: U.S. Geological Survey Open-File Report 93–198, 10 p., scale 1:50,000.

Miller, D.M., and Wooden, J.L., 1994, Field guide to Proterozoic geology of the New York, Ivanpah, and Providence Mountains, California: Field conference 1, Proterozoic orogenesis and metallogenesis project: U.S. Geological Survey Open-File Report 94-674, 51 p.

Murray, A.S., Marten, R., Johnston, A., and Martin, P., 1987, Analysis for naturally occurring radionuclides at environmental concentrations by gamma spectrometry: Journal of Radioanalytical and Nuclear Chemistry, Article 115, p. 263-288.

Prescott, J.R. and Hutton, J.T., 1994, Cosmic ray contributions to dose rates for luminescence and ESR dating: Large depths and long-term time variations: Radiation Measurements, v. 23, p. 497-500.

Reioux, D., Parrish, B., Swanson, B.J., and Brown, H.J., 2022a, Preliminary geologic map of the Pinto Valley 7.5' Quadrangle, New York Mountains, San Bernardino County, California: California Geological Survey, Preliminary Geologic Map 22-04, scale 1:24,000.

Reioux, D., Parrish, B., Swanson, B.J., and Brown, H.J., 2022b, Preliminary geologic map of the Ivanpah 7.5' Quadrangle, New York Mountains, San Bernardino County, California: California Geological Survey, Preliminary Geologic Map 22-03, scale 1:24,000.

Reioux, D., Parrish, B., Swanson, B.J., and Brown, H.J., 2022c, Preliminary geologic map of the Castle Peaks 7.5' Quadrangle, New York Mountains, San Bernardino County, California: California Geological Survey, Preliminary Geologic Map 22-01, scale 1:24,000.

Reioux, D., Parrish, B., Swanson, B.J., and Brown, H.J., 2022d, Preliminary geologic map of the Crescent Peak 7.5' Quadrangle, New York Mountains, San Bernardino County, California: California Geological Survey, Preliminary Geologic Map 22-02, scale 1:24,000.

Rollinson, H.R.,1993, Using geochemical data, evaluation, presentation, interpretation: Longman Scientific and Technical, Wiley, New York, 352 p.

Schwartz, J.J., Lackey, J.S., Miranda, E.A., Klepeis, K.A., Mora-Klepeis, G., Robles, F., and Bixler, J., 2023, Magmatic surge requires two-stage model for the Laramide Orogeny: Nature Communications, v. 14, no. 3841. https://doi.org/10.1038/s41467-023-39473-7

Snyder, S.L., and Duval, J.S., 2003, Design and construction of a gamma-ray spectrometer system for determining natural radioactive concentrations in geological samples at the U.S. Geological Survey in Reston, Virginia,: U.S. Geological Survey Open-File Report 03-29 (on-line only) (http://pubs.usgs.gov/of/2003/of03-029/).

Stacey, J., and Kramers, J.D. 1975, Approximation of terrestrial lead isotope evolution by a two-stage model: Earth and Planetary Science Letters, v. 26, p. 207-221.

Sun, S.S., and McDonough, W.F., 1989, Chemical and isotopic systematics of oceanic basalts: Implications for mantle composition and processes, in Saunders, A.D., and Norry, M.J., eds., Magmatism in the Ocean Basins: Geological Society, London, Special Publications, v. 42, 313-345.

Tera, F., and Wasserburg, G.J., 1972, U-Th-Pb systematics in three Apollo 14 basalts and the problem of initial Pb in lunar rocks: Earth and Plan¬etary Science Letters, v. 14, p. 281-304, https://doi.org/10.1016/0012-821X(72)90128-8.

Theodore, Ted G., 2007, Geology and mineral resources of the east Mojave National Scenic Area, San Bernardino County, California: U. S. Geological Survey Bulletin 2160. 265 p.

Vermeesch, P., 2018, IsoplotR: A free and open toolbox for geochronology: Geoscience Frontiers, v. 9, p. 1479-1493, https://doi.org/10.1016 /j.gsf.2018.04.001.

U.S. Geological Survey (USGS), 1984, USGS 1:24000-scale Quadrangle for Crescent Peak, Nevada-California, Provisional Edition 1984: U.S. Geological Survey.

U.S. Geological Survey (USGS), 2021, Geochemical data generated by projects funded by the USGS Earth Mapping Resources Initiative (ver. 12.0, December 2025): U.S. Geological Survey data release, https://doi.org/10.5066/P9WHRLXH.

Wintle, A.G., and Murray, A.S., 2006, A review of quartz optically stimulated luminescence characteristics and their relevance in single-aliquot regeneration dating protocols: Radiation Measurements, v. 41, p. 369-391.

Wooden, J.L., and Miller, D.M., 1990, Chronologic and isotopic framework for Early Proterozoic crustal evolution in the eastern Mojave Desert region, southeastern California: Journal of Geophysical Research, v. 95, no. B12, p. 20,133-20,146.

AUTHORSHIP DOCUMENTATION AND PRODUCT LIMITATIONS

PUBLICATION TITLE: Geochronology and Geochemistry Data Release for the New York Mountains Earth MRI Project, San Bernardino County, California: U-Pb Radiometric Dating, Luminescence Dating, Geochemistry

Data Release 2026-01

LIMITATIONS: The data contained in this data release report were provided by the noted laboratories based on their expertise and the California Department of Conservation makes no warranties as to the reported results or their suitability for any given purpose.

First Author – Brian J. Swanson (CGS), PG No. 6494, CEG No. 2055

Date: July 8, 2026

Expires 6/30/2028

Second Author – David Reioux (CGS), PG No.9462

Date: July 8, 2026

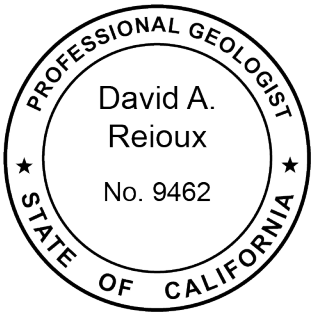

Expires 2/29/2028

Third Author – Benjamin M. Parrish (CGS), PG No. 9609

Date: July 8, 2026

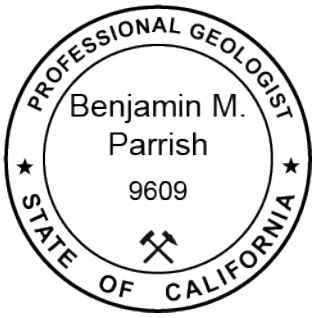

Expires 7/31/2028

Fourth Author – Matthew J. Towne, Assistant Geologist (CGS)

Fifth Author – Dr. Joshua J. Schwartz, U-Pb Dating Geochronologist (CSUN)

Sixth Author – Shannon A. Mahan, Luminescence Dating Geochronologist (USGS)

Work in Responsible Charge: Data compilation, research, evaluation of sample locations, field identification of geologic units, development of sampling protocol, and map generation by CGS geologists and geochronology data and interpretations by Joshua Schwartz and Shannon Mahan.

This authorship document accompanies DR 2026-01 with the following citation. When using data that accompanies this document, reference this citation:

Swanson, B.J., Reioux, D., Parrish, B.M., Towne, M.J., Schwartz, J.J., and Mahan, S.A., 2026, Geochronology and geochemistry data release for the New York Mountains Earth MRI project, San Bernardino County, California: U-Pb radiometric dating, luminescence dating, geochemistry: California Geological Survey Data Release, DR 2026-1, 18 p., Appendices A, B, and C, Supplemental Geochronology and Geochemistry Data.

APPENDIX A: GEOLOGIC DETAIL MAPS OF SAMPLE LOCATIONS

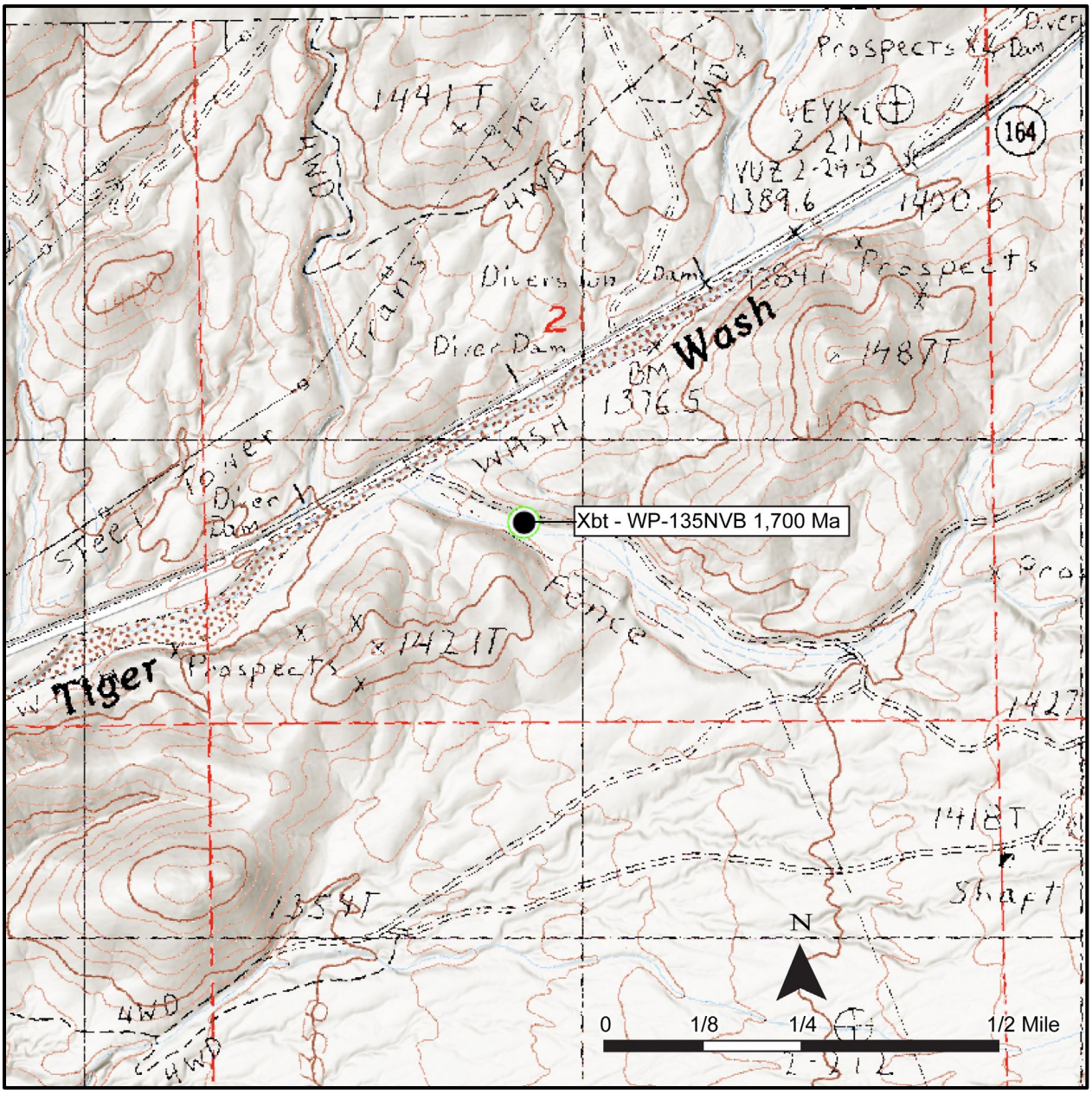

Figure A1. Nevada Crescent Peak Quadrangle Detail Map 1

Locations of sample point WP-135NVB adjacent to Big Tiger Wash in Nevada shown on an extracted portion of the Crecent Peak Quadrangle topographic map (USGS, 1984). Refer to figure 1 for point symbology.

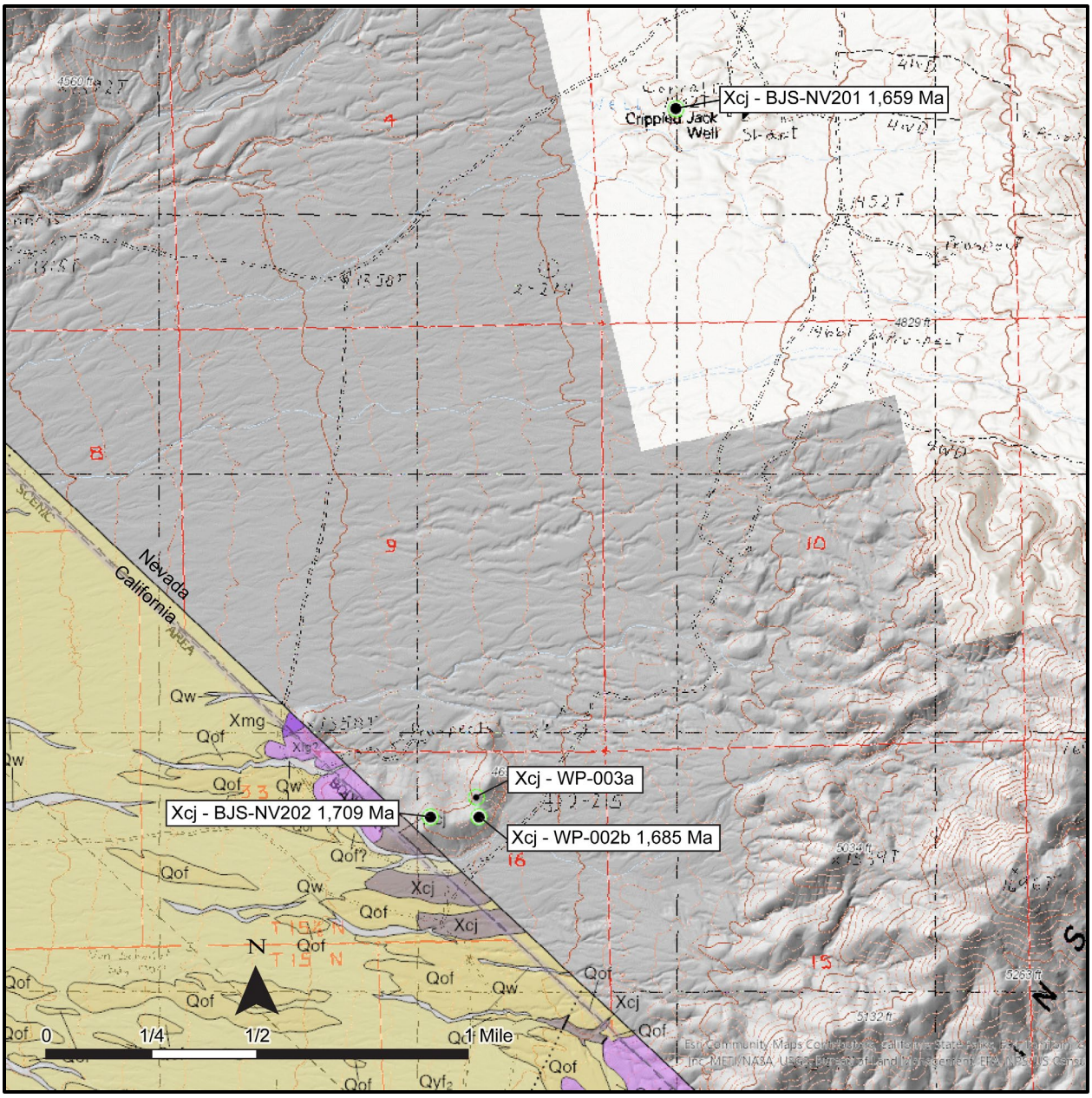

Figure A2. Nevada Crescent Peak Quadrangle Detail Map 2

Location of sample points BJS-NV201, BJS-NV202, WP-002b, and WP-003a in Nevada shown on an extracted portion of the Crecent Peak Quadrangle topographic map (USGS, 1984) and portion of geologic map (Reioux and others, 2022d). Refer to figure 1 for point symbology.

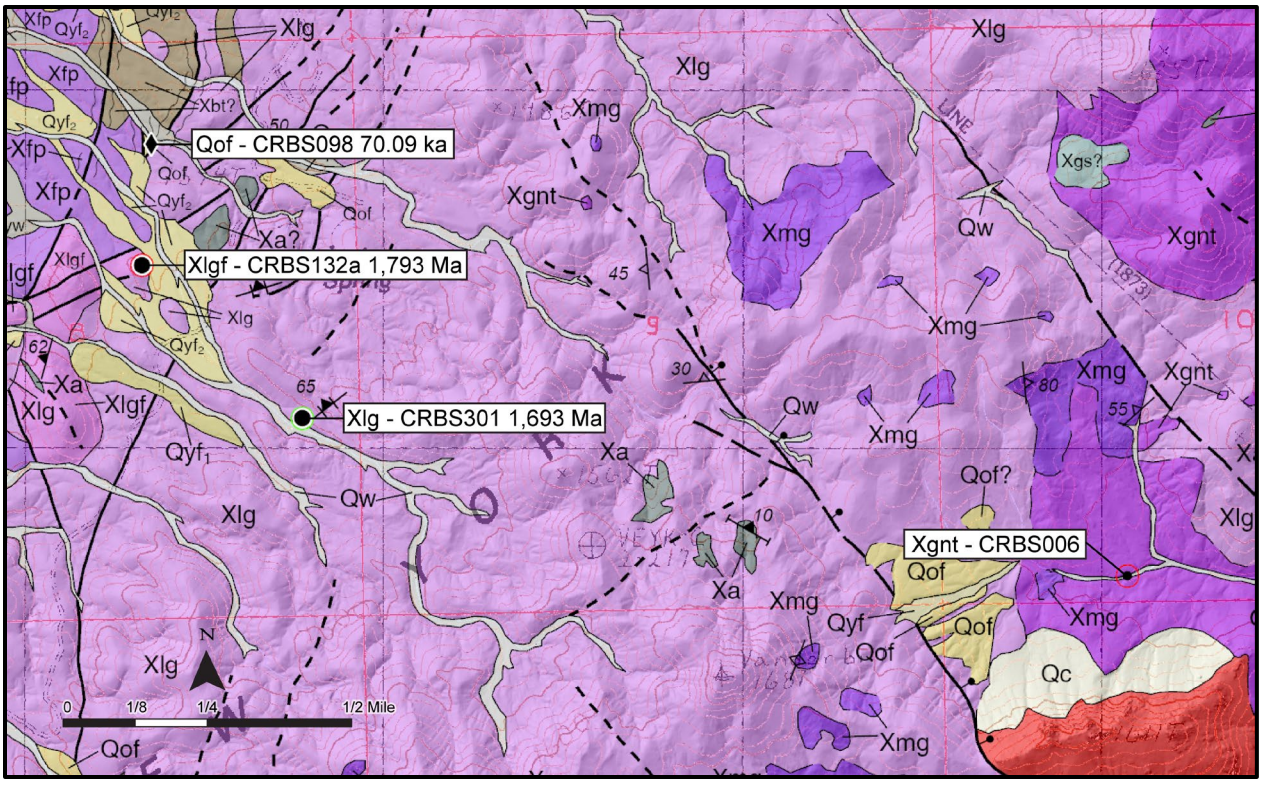

Figure A3. Crescent Peak Quadrangle Detail Map 1

Location of sample points CRBS098, CRBS132a, CRBS301, and CRBS006 shown on an extracted portion of the Crecent Peak Quadrangle geologic map (Reioux and others, 2022d). Refer to figure 1 for point symbology.

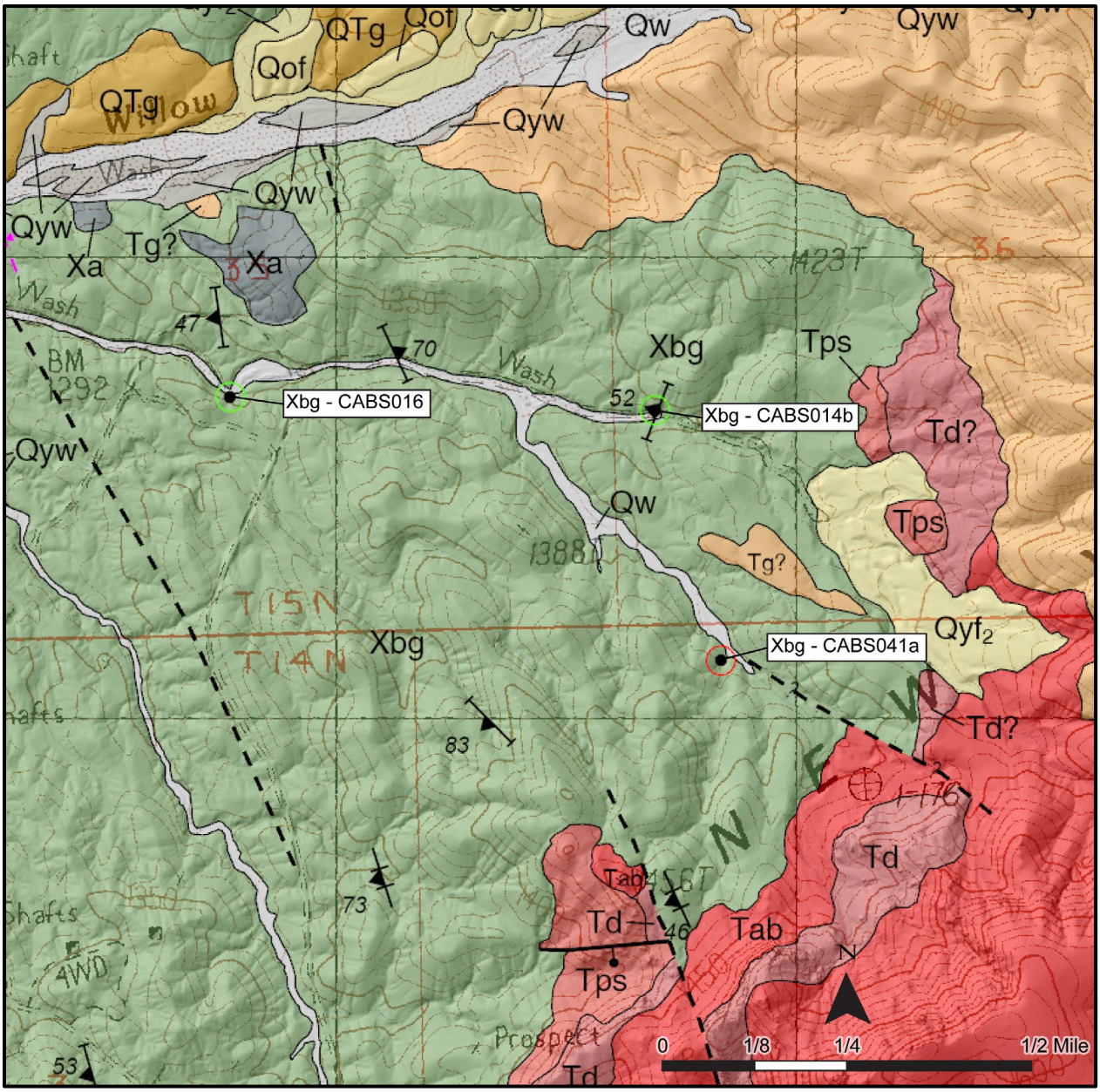

Figure A4. Castle Peaks Quadrangle Detail Map 1

Location of sample points CABS016, CABS014b, and CABS014a shown on an extracted portion of the Castle Peaks Quadrangle geologic map (Reioux and others, 2022c). Refer to figure 1 for point symbology.

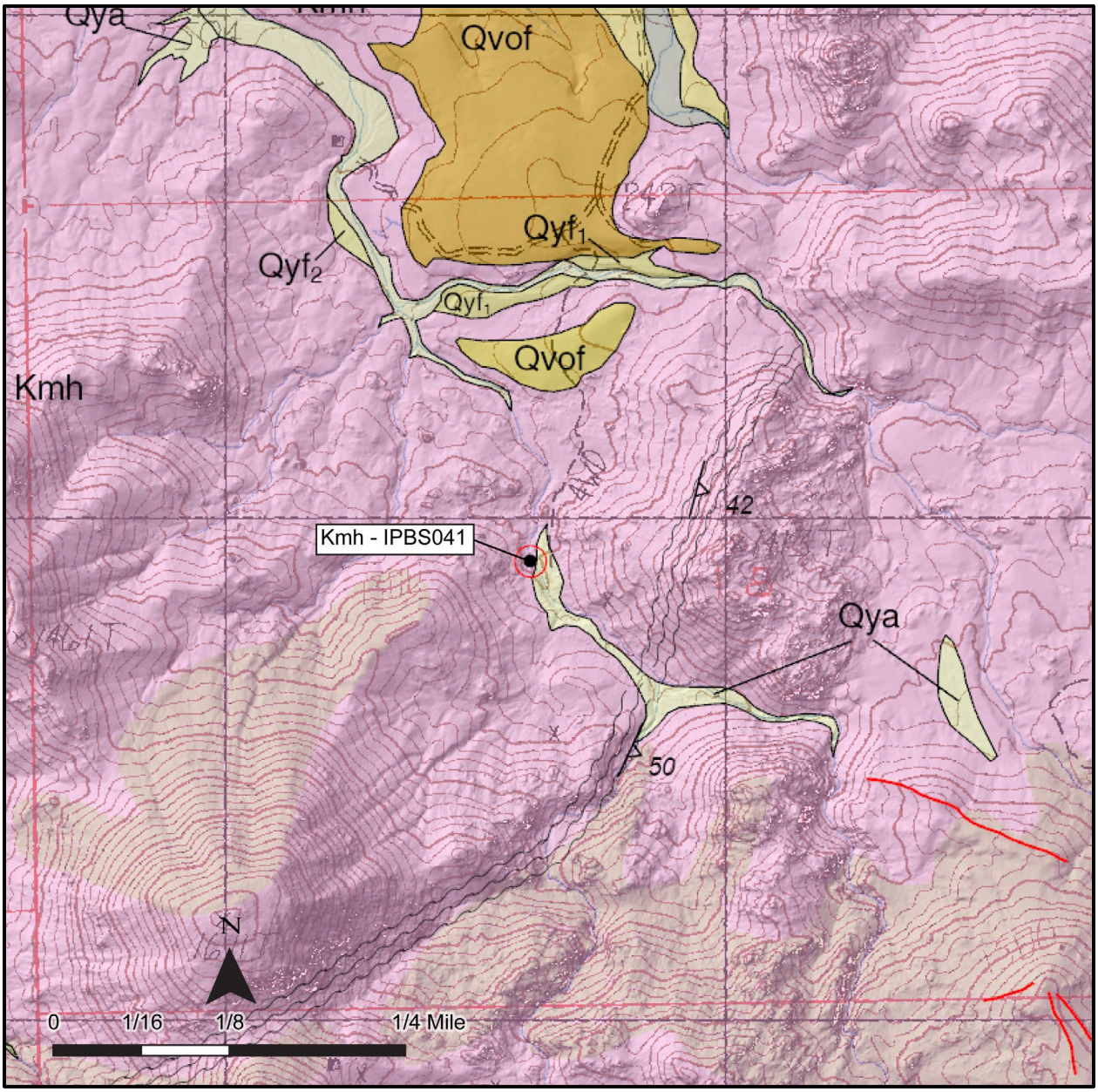

Figure A5. Ivanpah Quadrangle Detail Map 1

Location of sample point IPBS041 shown on extracted portion of the Ivanpah Quadrangle geologic map (Reioux and other, 2022b). Refer to figure 1 for point symbology.

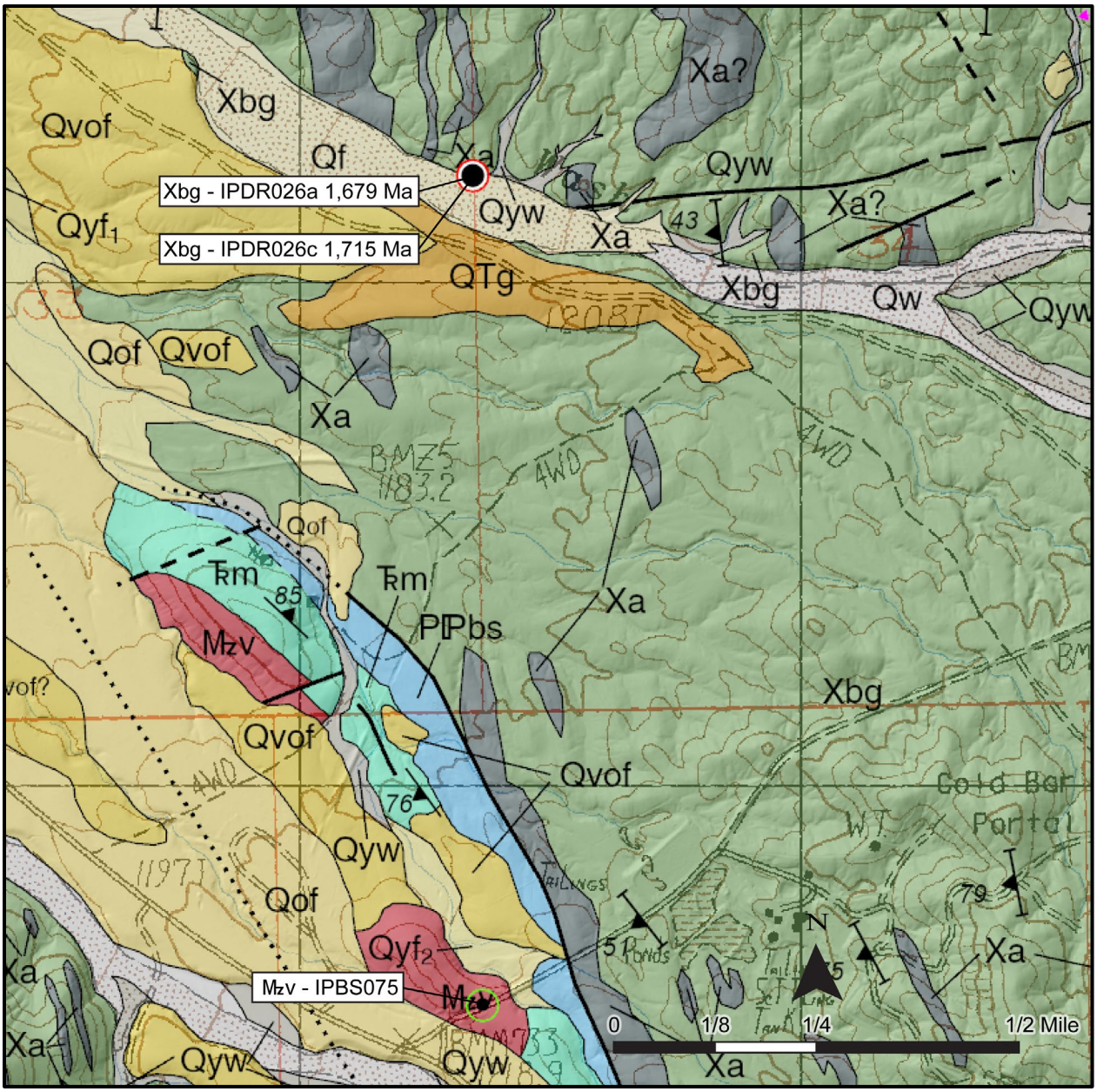

Figure A6. Ivanpah Quadrangle Detail Map 2

Location of sample points IPDR026a, IPDR026c, and IPBS075 shown on an extracted portion of the Ivanpah Quadrangle geologic map (Reioux and others, 2022b). Refer to figure 1 for point symbology.

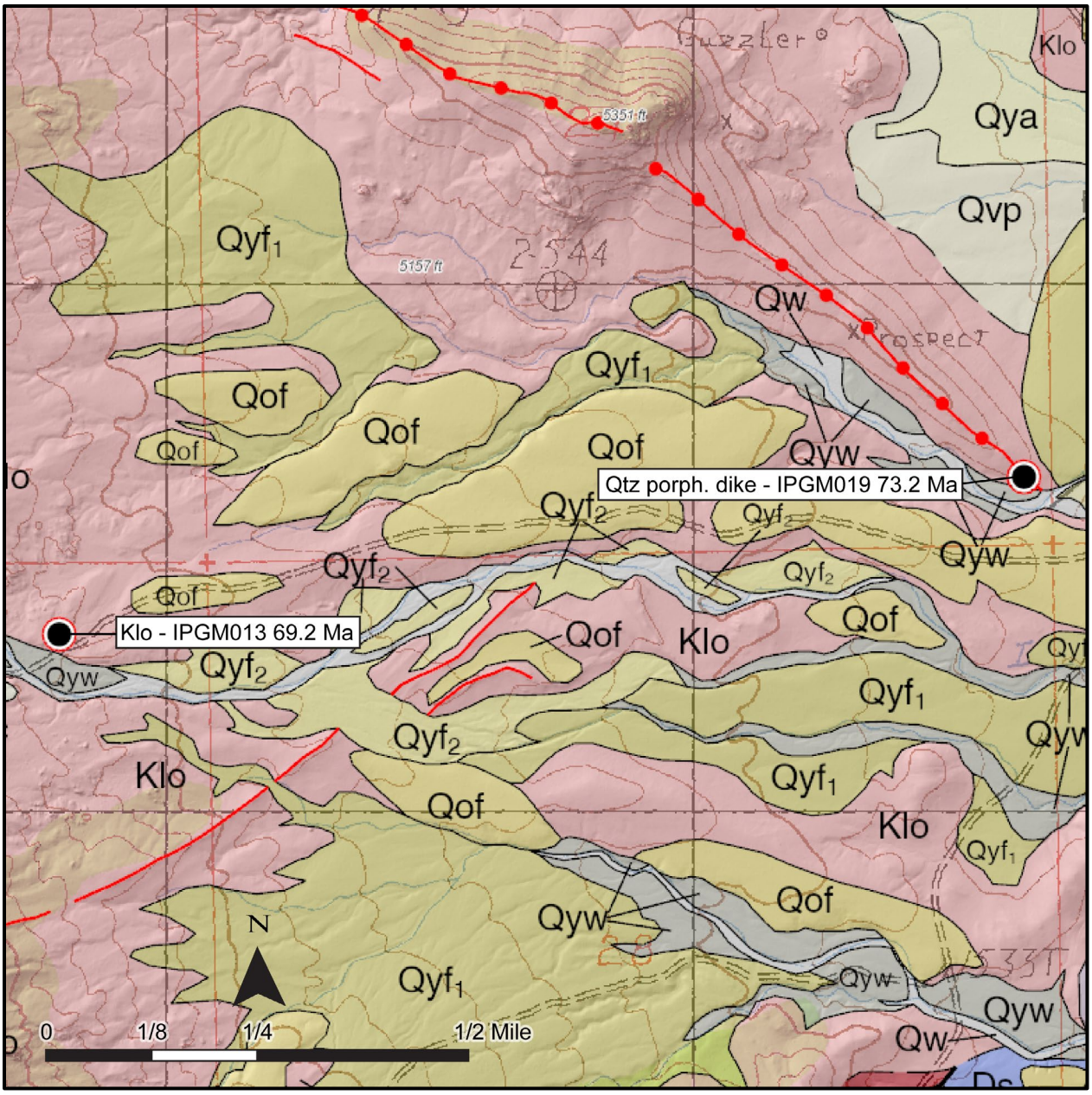

Figure A7. Ivanpah Quadrangle Detail Map 3

Location of sample points IPGM013 and IPGM019 shown on an extracted portion of the Ivanpah Quadrangle geologic map (Reioux and others, 2022b). Refer to figure 1 for point symbology.

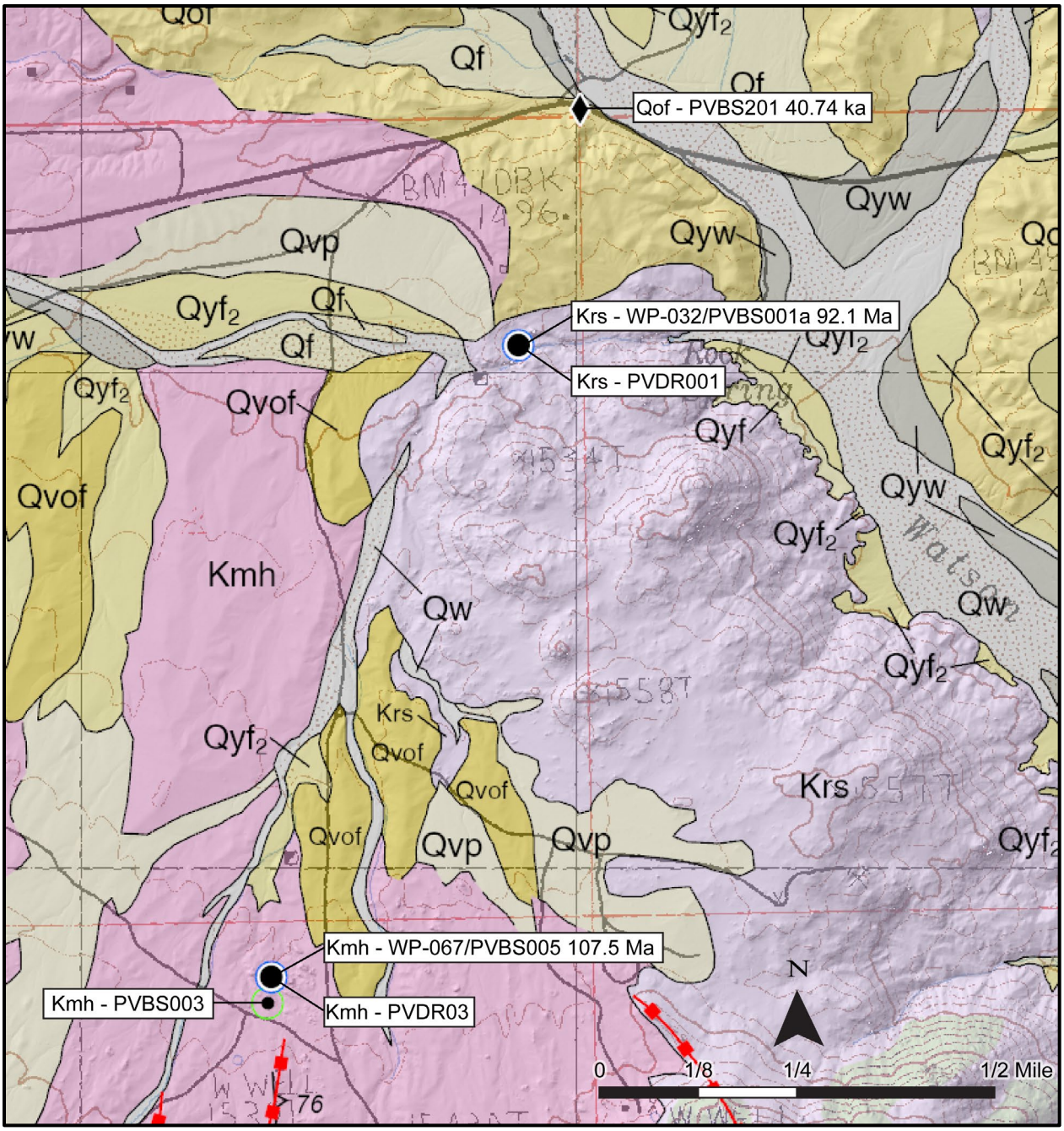

Figure A8. Pinto Valley Quadrangle Detail Map 1

Location of sample points PVBS201, WP-032 (PVBS001a), PVDR001, WP-067, PVBS003, and PVDR03 shown on an extracted portion of the Pinto Valley Quadrangle geologic map (Reioux and others, 2022a). Refer to figure 1 for point symbology.

APPENDIX B: GEOCHRONOLOGY PLOTS, SAMPLE PHOTOGRAPHS, AND DISCUSSION

Uranium-Lead Dating:

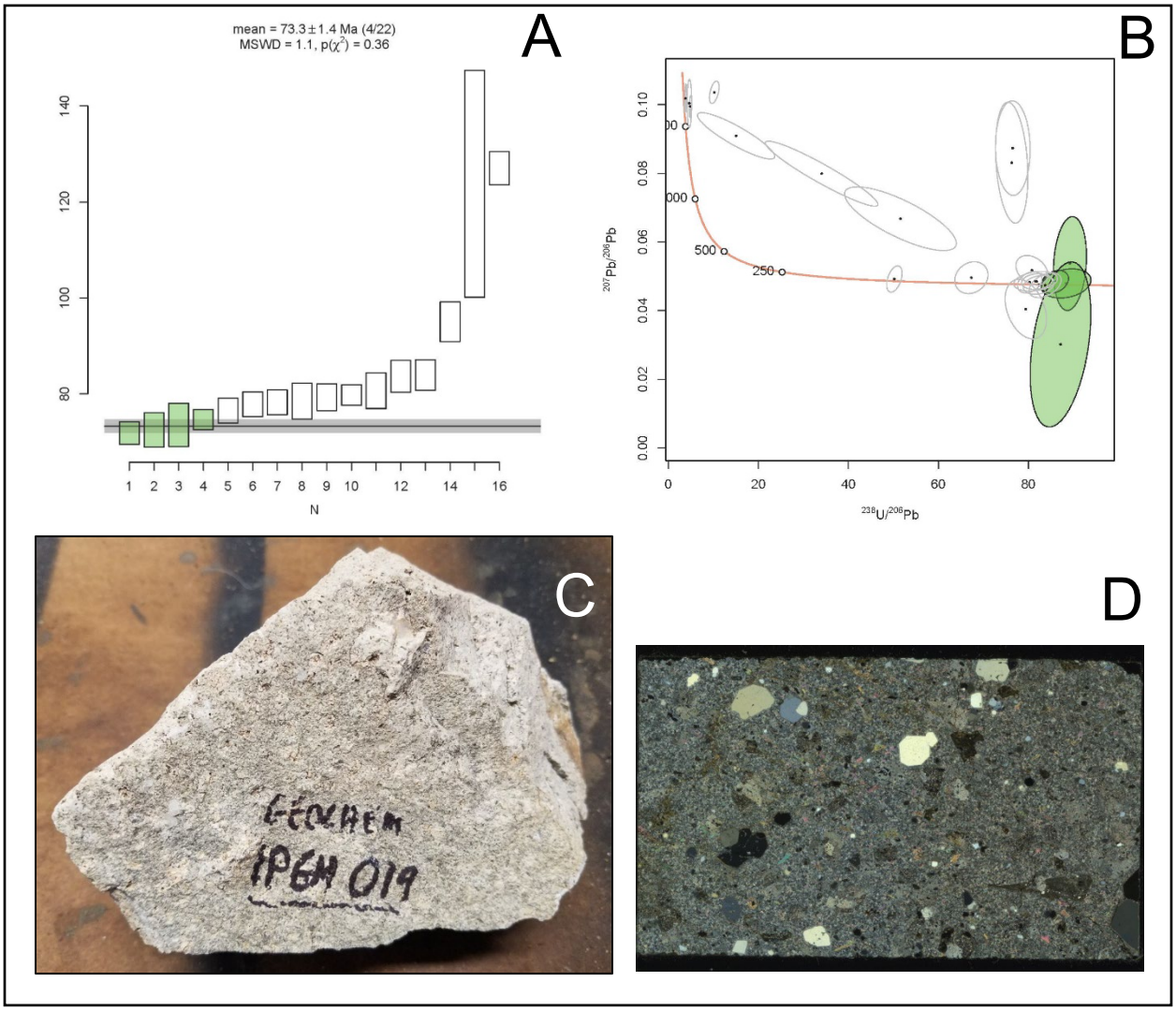

Figure B1. Sample IPGM019

Quartz porphyry dike cutting Live Oak Pluton (Klo): (A) ^{207}Pb-corrected $^{206}Pb/^{238}U$ zircon dates, (B) Tera-Wasserburg concordia plot, (C) Sample photograph, and (D) Photomicrograph of thin section (crossed polarized light). Maximum mean age of 73.3 ±1.4 [2.0] Ma, MSWD = 1.1 reported based on U-Pb dating of the youngest 4 of 22 zircons obtained from the sample; concordia plot indicates upper intercept age of 1,625-1,670 Ma for inherited zircons. Note that even the youngest four zircons are older than the age reported for the Klo host rock that the dike cuts (sample IPGM013 – 69.2 Ma). This suggests that even these youngest zircons could be inherited from the host rock rather than the true crystallization age of this cross-cutting dike. Burchfiel and Davis (1977) reported a minimum K-Ar age of 71.7 ±0.8 for the quartz porphyry dikes.

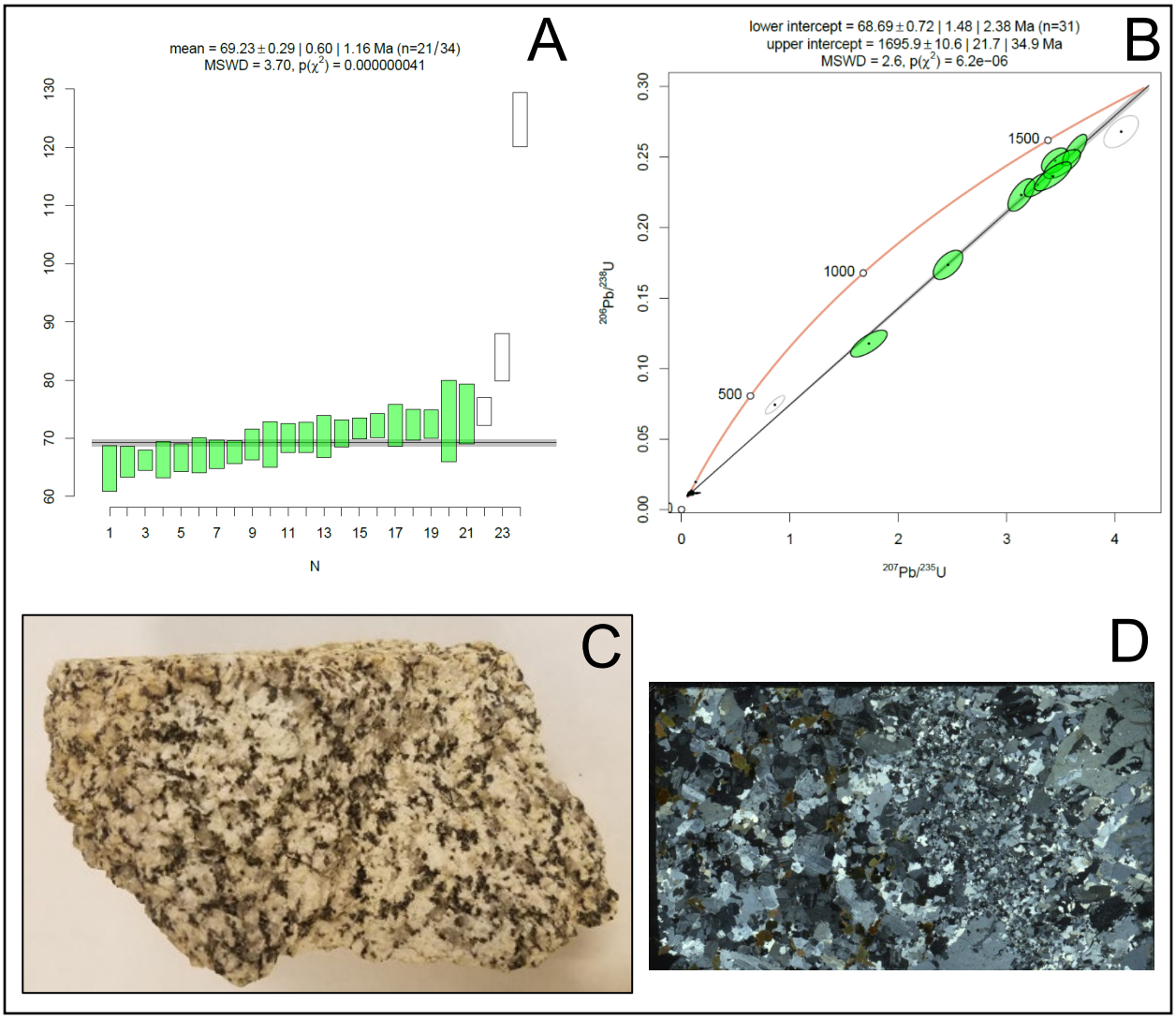

Figure B2. Sample IPGM013

Live Oak Pluton (Klo): (A) ^{207}Pb-corrected $^{206}Pb/^{238}U$ zircon dates, (B) Conventional concordia plot, (C) Sample photograph, and (D) Photomicrograph of thin section (crossed polars). Mean age of 69.2 ±0.6 [1.5] Ma, MSWD = 3.7 reported based on U-Pb dating of 21 of 34 zircons obtained from the sample; concordia plot indicates upper intercept age of about 1,696 Ma for inherited zircons. Beckerman (1982) previously reported an age of 79.9 ±2.4 Ma based on K-Ar dating of biotite. The apparent conflict between the previously reported older K-Ar date and the older date we obtained for the quartz porphyry dike that cuts Klo regionally suggests that IPGM013 may have sampled a younger porphyritic phase of Klo; alternatively, the zircons in IPGM019 may all be inherited and the true age of crystallization is unrecorded in our analyses but younger than 69.2 Ma.

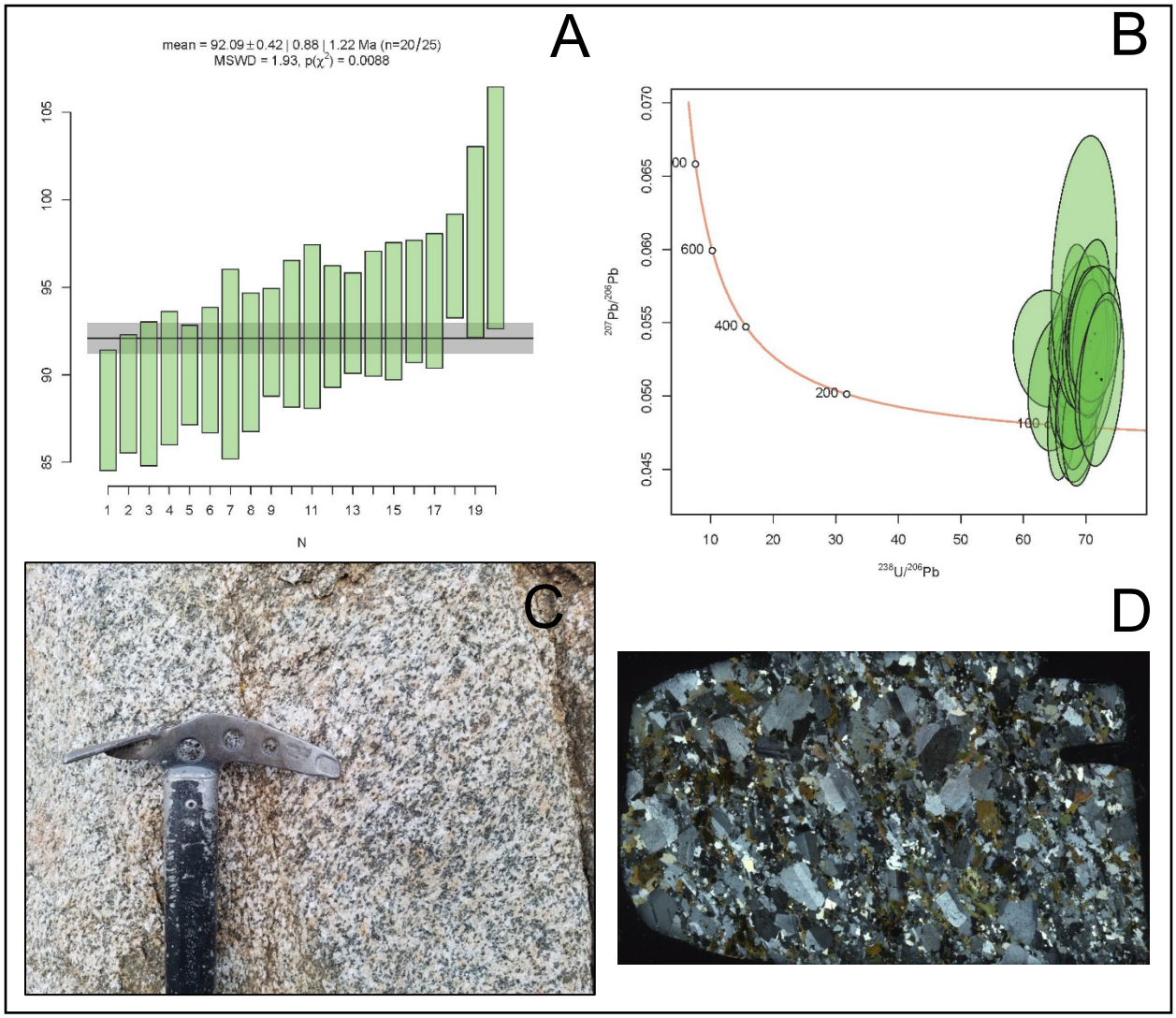

Figure B3. Sample WP-032

Rock Springs Pluton (Krs): (A) ^{207}Pb-corrected $^{206}Pb/^{238}U$ zircon dates, (B) Tera-Wasserburg concordia plot, (C) Outcrop photograph, and (D) Photomicrograph of thin section (crossed polars). Mean age of 92.1 ±0.9 [2.1] Ma, MSWD = 1.9 reported based on U-Pb dating of 20 of 25 zircons obtained from the sample; concordia plot indicates no inherited Proterozoic zircons, perhaps corresponding to the lack of Proterozoic rocks mapped on the southwest side of the Slaughterhouse fault. U-Pb dating of titanites yielded a tentative older age of 113.7 ±0.4 [2.3] Ma, MSWD = 5.2. Previous U-Pb dating yielded an age of about 97 Ma (Ed Dewitt, 1985 oral commun., in Theodore (2007)).

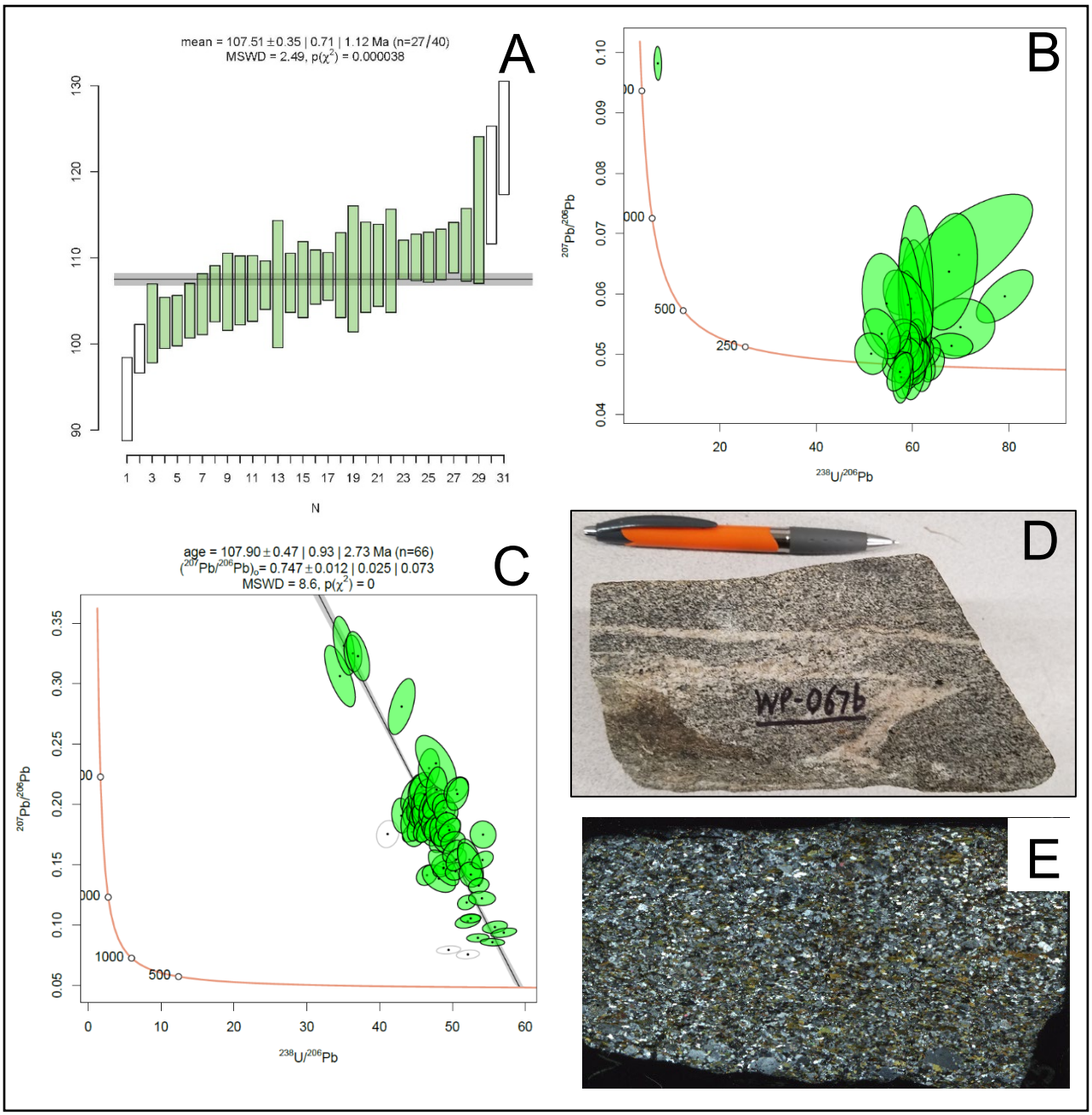

Figure B4. Sample for WP-067 (WP-67b)

Hornblende granodiorite enclave in Rock Springs Pluton: (A) ^{207}Pb-corrected $^{206}Pb/^{238}U$ zircon dates, (B) Tera-Wasserburg concordia plot showing zircons, (C) Tera-Wasserburg concordia plot showing titanite discordia array, (D) Sample photograph, and (E) Photomicrograph of thin section. Mean age of 107.5 ±0.7 [2.3] Ma, MSWD = 2.5 reported based on U-Pb dating of 27 of 40 zircons obtained from the sample; only one inherited zircon found. U-Pb dating of titanites yielded a nearly identical age of 107.9 ±0.9 [2.2] Ma, MSWD = 8.6.

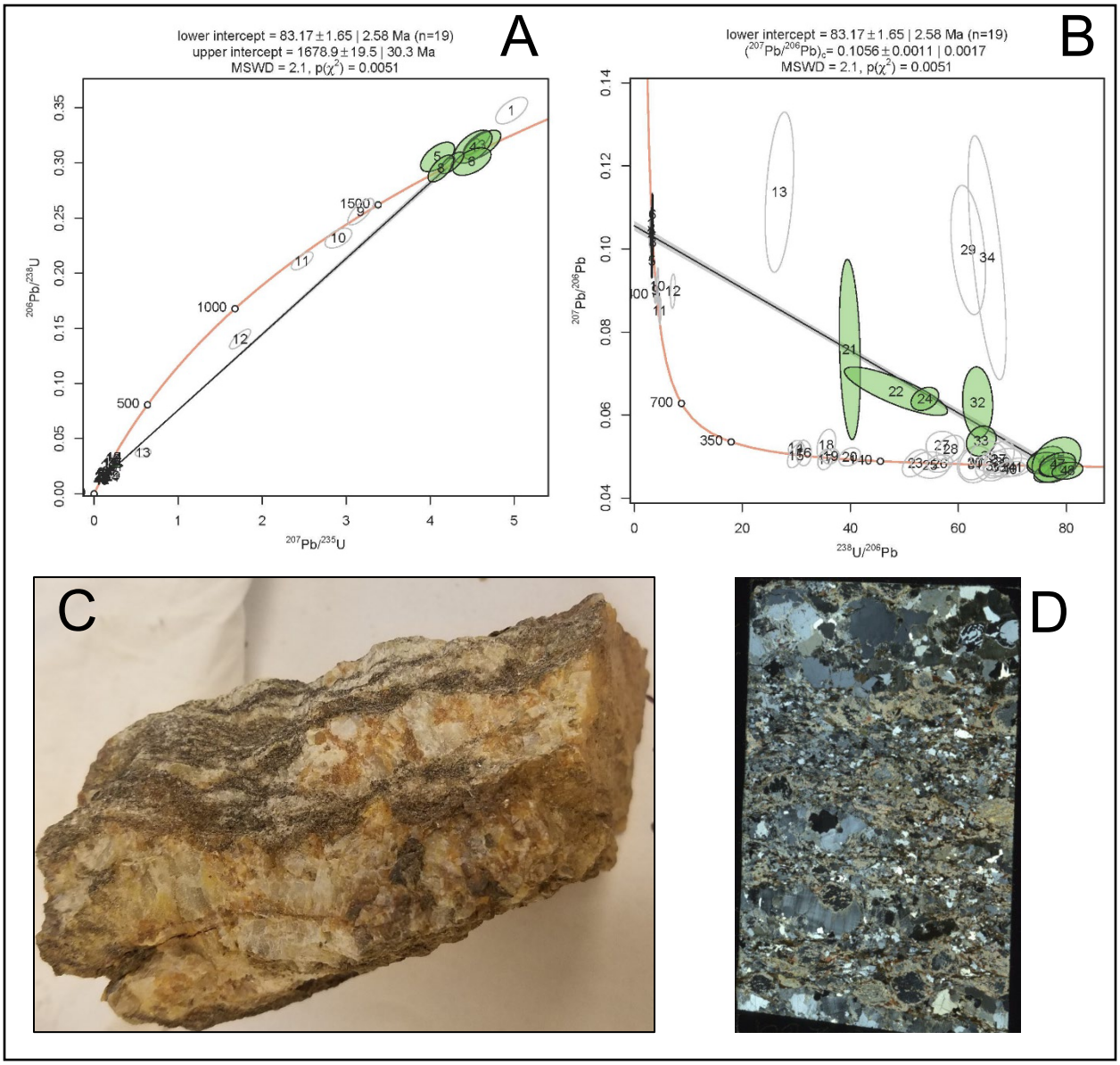

Figure B5. Sample IPDR026a

Biotite gneiss of Willow Wash (Xbg): (A) Conventional concordia plot, (B) Tera-Wasserburg concordia plot, (C) Sample photograph, and (D) Photomicrograph of thin section (crossed polars). Upper intercept age of 1,679 ±30 [45] Ma, MSWD = 2.1 reported based on U-Pb dating of 19 of 50 zircons obtained from the sample. The lower intercept date of 83.2 Ma is intermediate between the ages reported for the Rock Springs Pluton (92.1 Ma) and the younger Live Oak Pluton (69.2 Ma). Miller and Wooden (1994) previously reported U-Pb and Pb-Pb ages of zircons ranging from 1.7 Ga to 1.9 Ga for this gneiss.

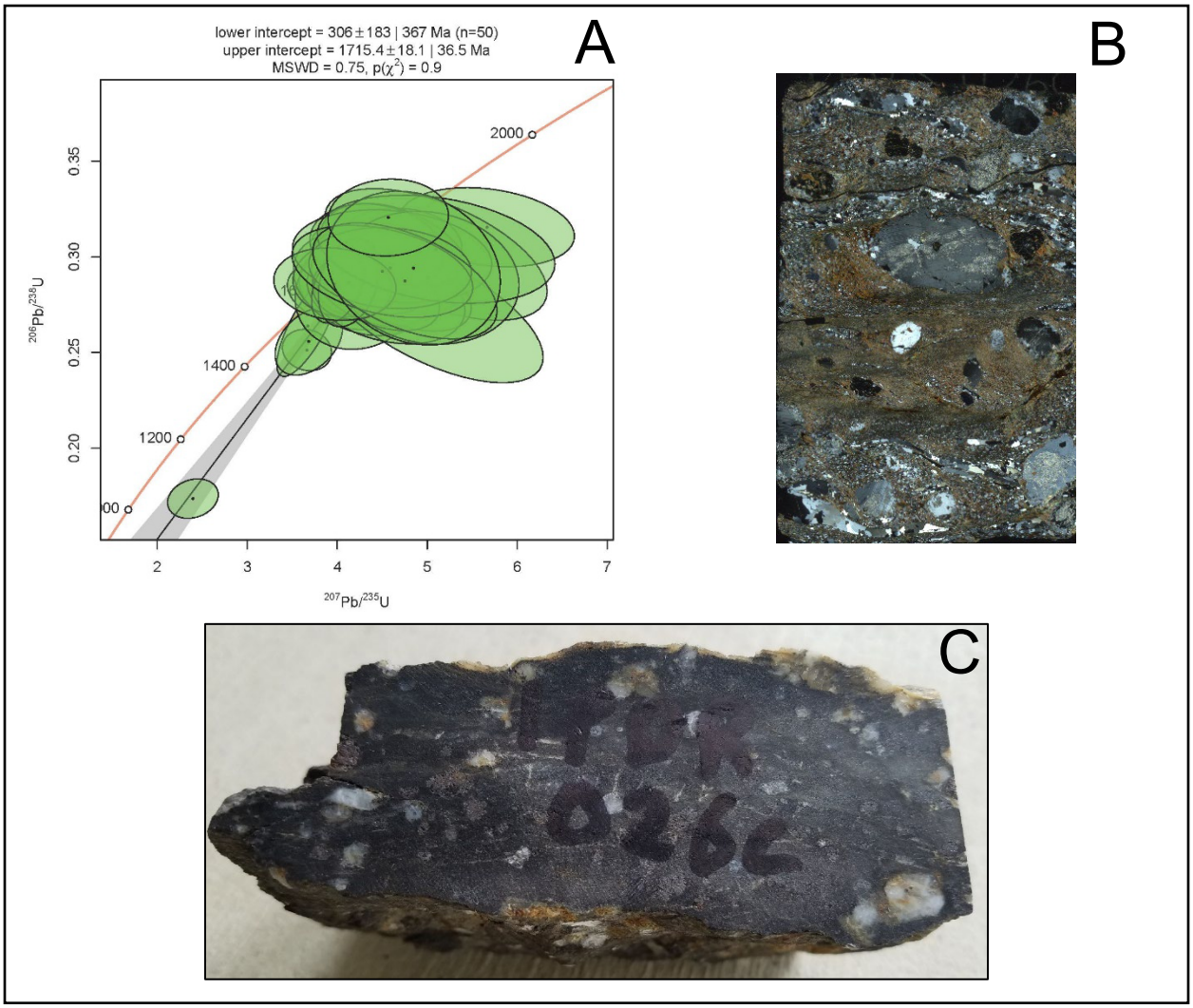

Figure B6. Sample IPDR026c

Fine-grained porphyry/augen gneiss mapped within biotite gneiss of Willow Wash (Xbg); similar to Xfp unit mapped in the Crescent Peak Quadrangle and commonly overprinted by mylonitic texture: (A) Conventional concordia plot, (B) Photomicrograph of thin section (crossed polars), (C) Sample photograph. Upper intercept age 1,715 ±37 [50] Ma; MSWD = 0.75, reported based on U-Pb dating of 50 of 50 zircons obtained from the sample. Note the low MSWD value and tight cluster near the concordia line suggesting a magmatic origin and the zircons did not experience much lead loss.

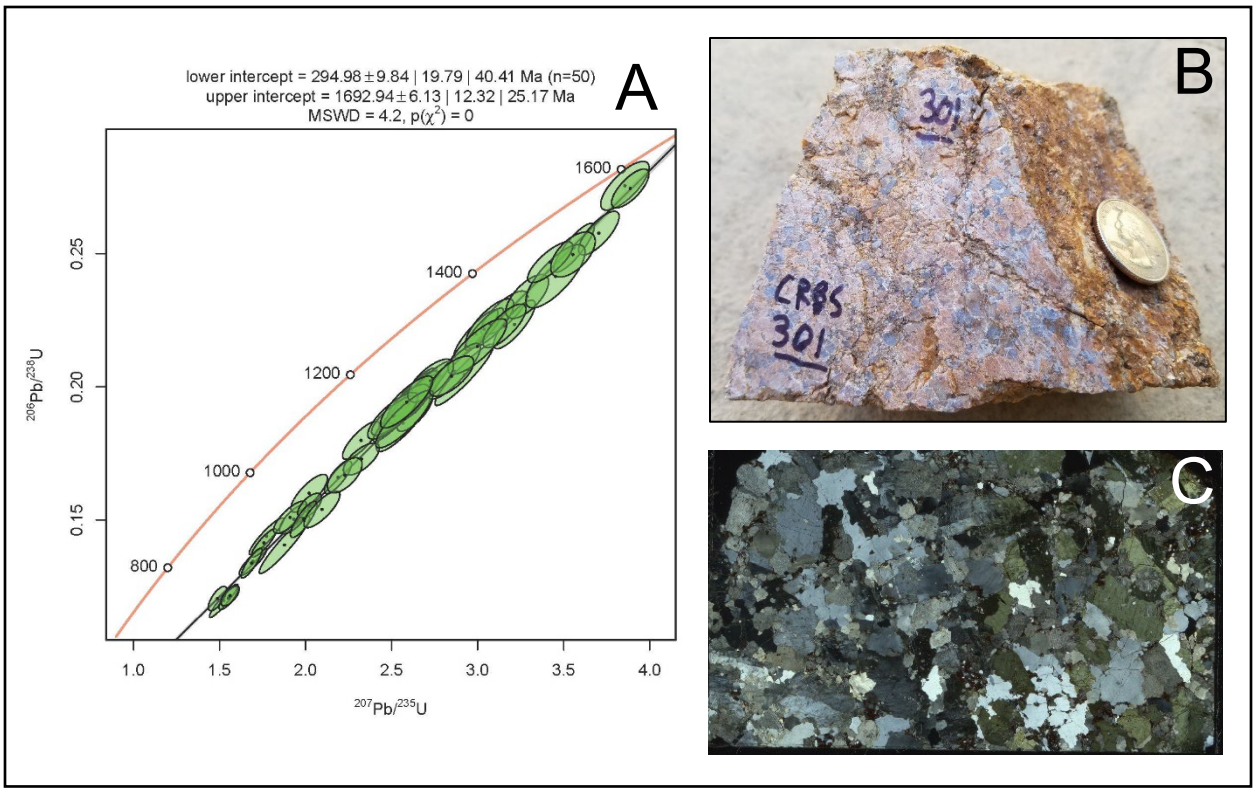

Figure B7. Sample CRBS301

Leucogranite (Xlg): (A) Conventional concordia plot, (B) Sample photograph, (C) Photomicrograph of thin section (crossed polars). Mean age 1,693 ±12 [36] Ma; MSWD = 4.2, reported based on U-Pb dating of 50 of 50 zircons obtained from the sample. Note that the zircons are generally discordant due to lead loss, resulting in a lower intercept age of about 295 Ma. Miller and Wooden (1993) previously reported U-Pb ages ranging from 1,672 to 1,695 Ma for the New York Mountains leucogranite.

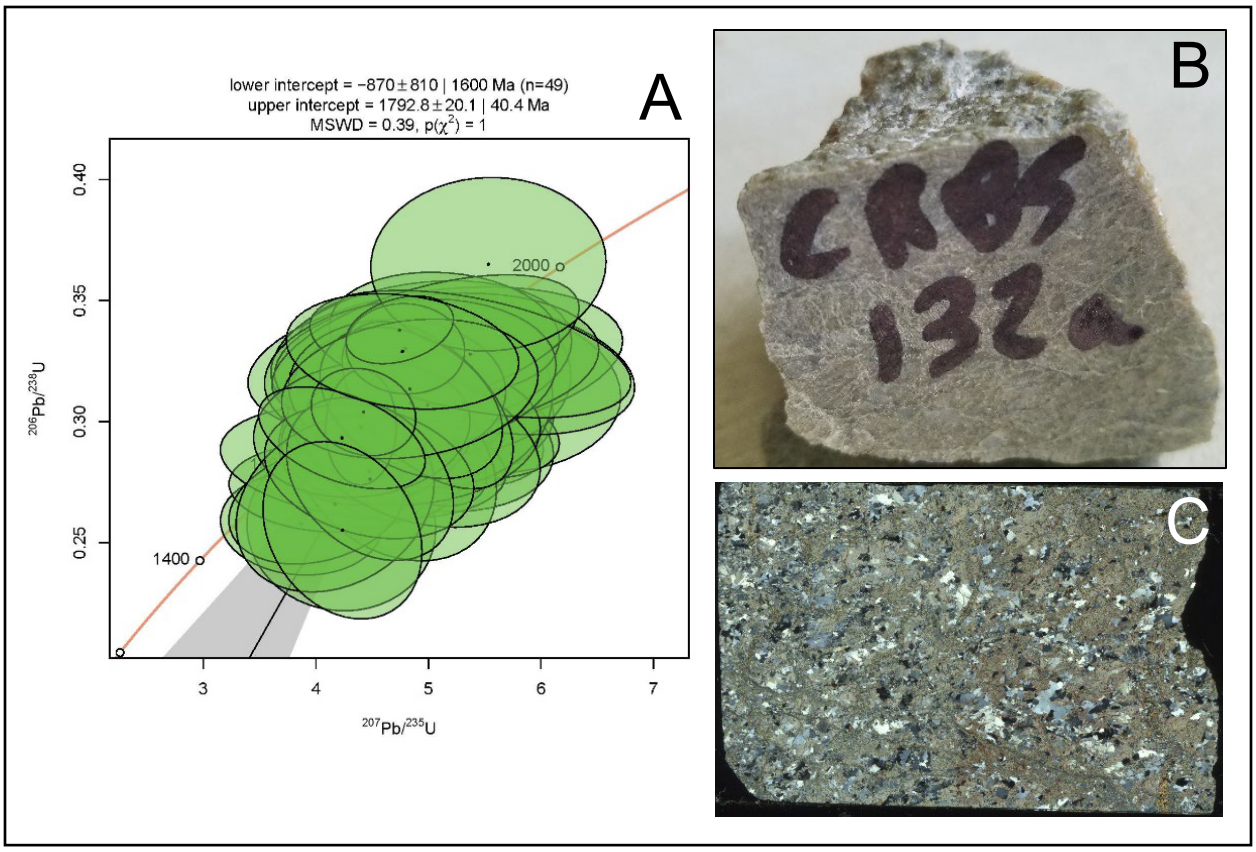

Figure B8. Sample CRBS132a

Fine grained, porphyritic, meta-volcanic rock (Xlgf): (A) Conventional concordia plot, (B) Sample photograph, and (C) Photomicrograph of thin section (crossed polars). Upper intercept age of 1,793 ±40 [54] Ma; MSWD = 0.4, reported based on U-Pb dating of 49 of 50 zircons obtained from the sample. Note the low MSWD value and tight cluster near the concordia line suggesting a magmatic (volcanic) origin and the zircons did not experience much lead loss. This unit subdivided from the leucogranite of Miller and Wooden (1993), who previously reported U-Pb ages ranging from 1,672 to 1,695 Ma for the leucogranite.

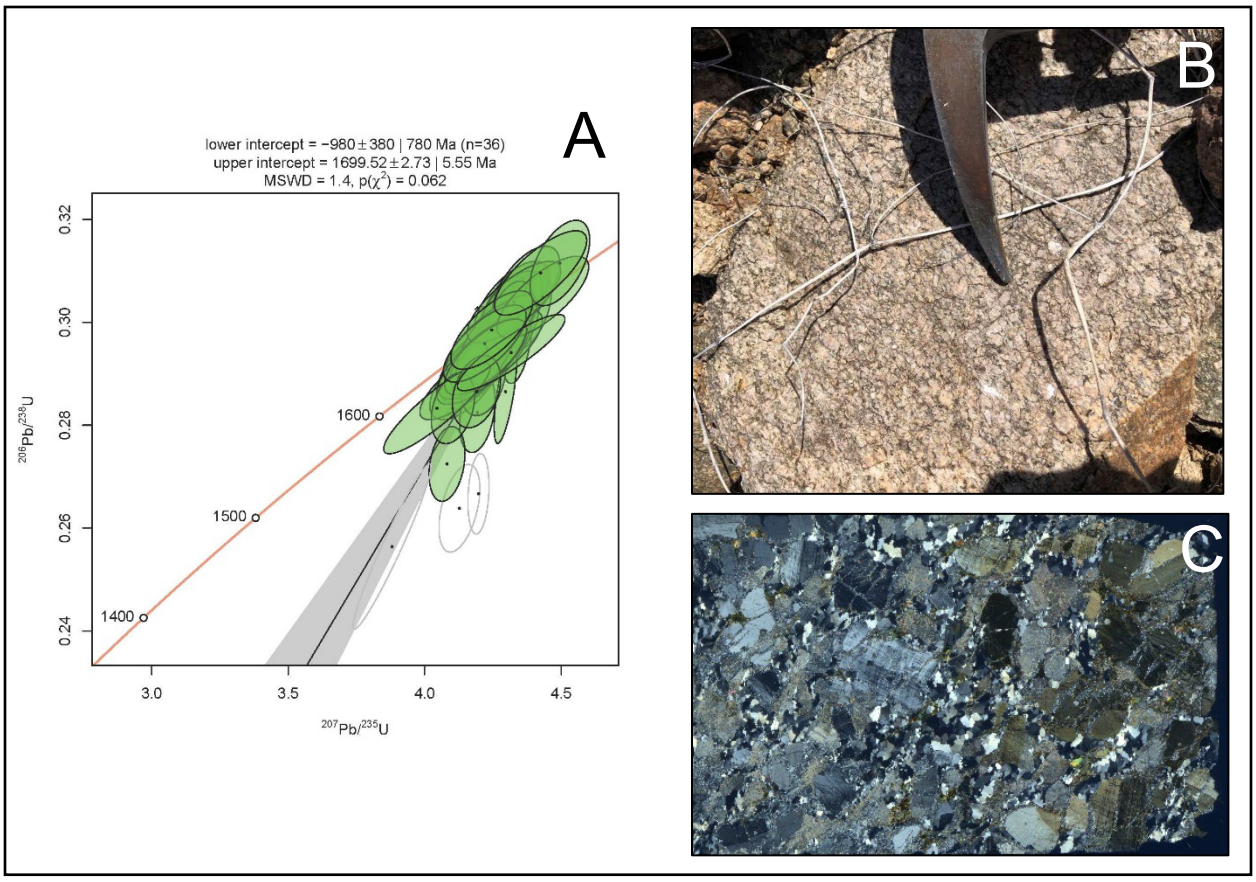

Figure B9. Sample WP-135NVb

Granodiorite of Big Tiger Wash - Leucocratic porphyritic phase (Xbt): (A) Conventional concordia plot, (B) Sample photograph, and (C) Photomicrograph of thin section (crossed polars). Upper intercept age of 1,700 ±6 [34] Ma; MSWD = 1.4, reported based on U-Pb dating of 36 of 40 zircons obtained from the sample. Note the low MSWD value and tight cluster near the concordia line confirming a magmatic origin and the zircons did not experience much lead loss. Wooden and Miller (1990) previously reported a U-Pb age of approximately 1,675 Ma for this unit.

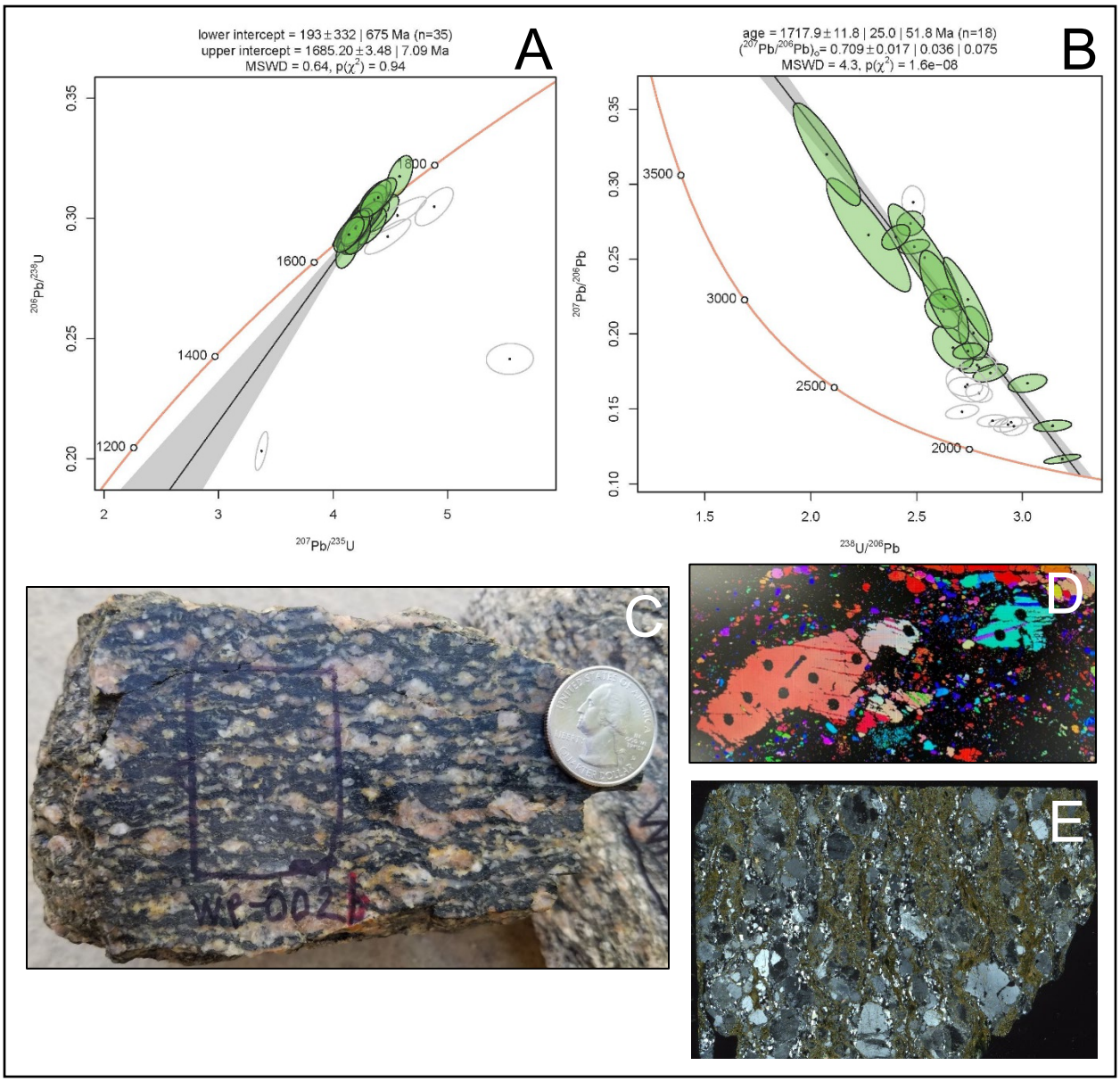

Figure B10. Sample WP-002b

Granodiorite of Crippled Jack Well with mylonitic texture (Xcj): (A) Conventional concordia plot showing zircon analyses, (B) Tera-Wasserburg plot showing titanite analyses and a discordia array, (C) Sample photograph, (D) Electron Backscatter Diffraction (EBSD) image showing example of dated titanites and laser spots (E) Photomicrograph of thin section (crossed polars). Upper intercept age of 1,685 ±7 [34] Ma; MSWD = 0.6, reported based on U-Pb dating of 35 of 40 zircons obtained from the sample. Note the low MSWD value and tight cluster near the concordia line confirming a magmatic origin and the zircons did not experience much lead loss. U-Pb dating of titanites yielded an anomalously older age of about 1718 Ma based on the youngest 18 of 28 titanite ages, with an MSWD of 4.3; incorporation of all titanite ages yielded an older age of about 1815 Ma. Miller and Wooden (1994) previously reported a UPb date of 1659 ±4 Ma on zircon collected at Moore siding (resampled at BJS-NV202) and a second UPb date of 1,662 ±7 Ma was obtained near the type locality (type area resampled at BJS-NV201) of the pluton (Miller written commun., Dec. 2021), both based on TIMS analyses.

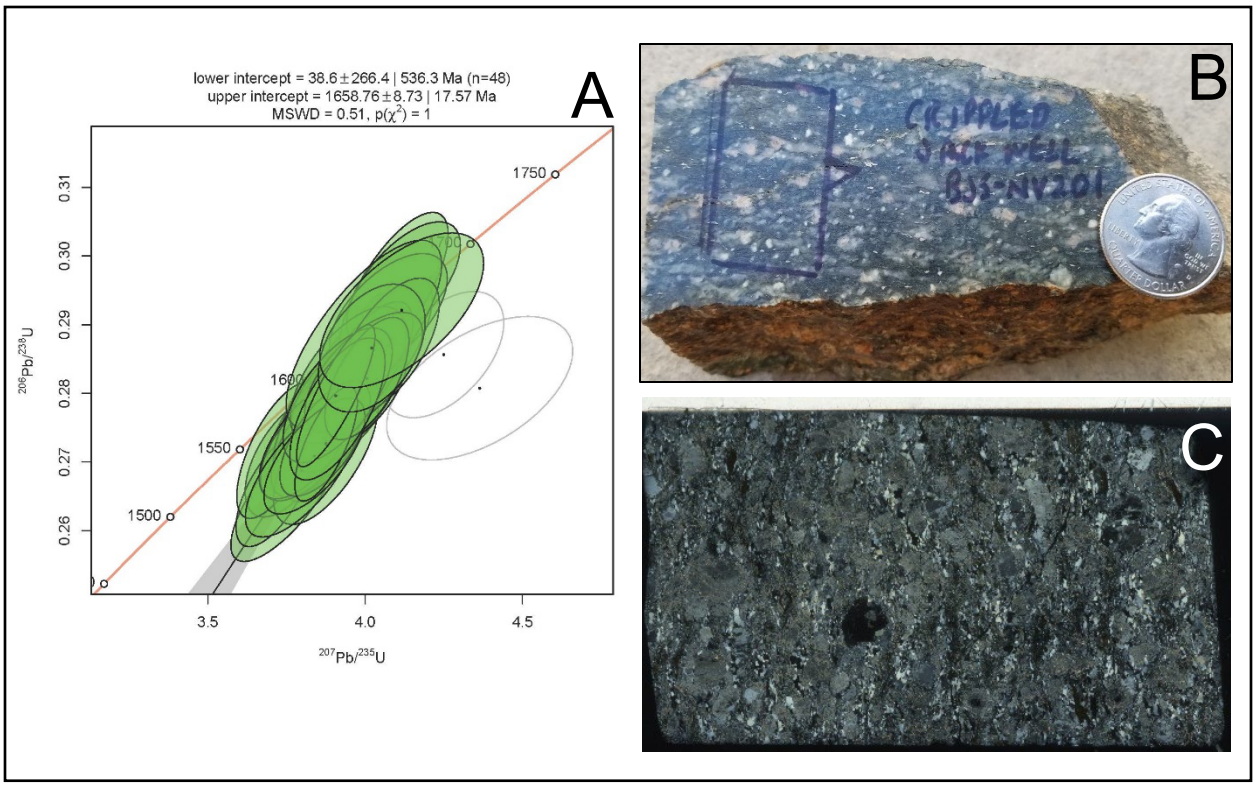

Figure B11. Sample BJS-NV201

Granodiorite of Crippled Jack Well with mylonitic texture, sampled near Crippled Jack Well (Xcj): (A) Conventional concordia plot showing zircon analyses, (B) Sample photograph, (C) Photomicrograph of thin section (crossed polars). Upper intercept age of 1,659 ±17 [37] Ma; MSWD = 0.5, reported based on U-Pb dating of 48 of 50 zircons obtained from the sample. Note the low MSWD value and tight cluster near the concordia line confirming a magmatic origin and the zircons did not experience much lead loss. A U-Pb date of 1,662 ±7 Ma was previously obtained near the type locality of the pluton (Miller written commun., Dec. 2021), based on TIMS analyses.

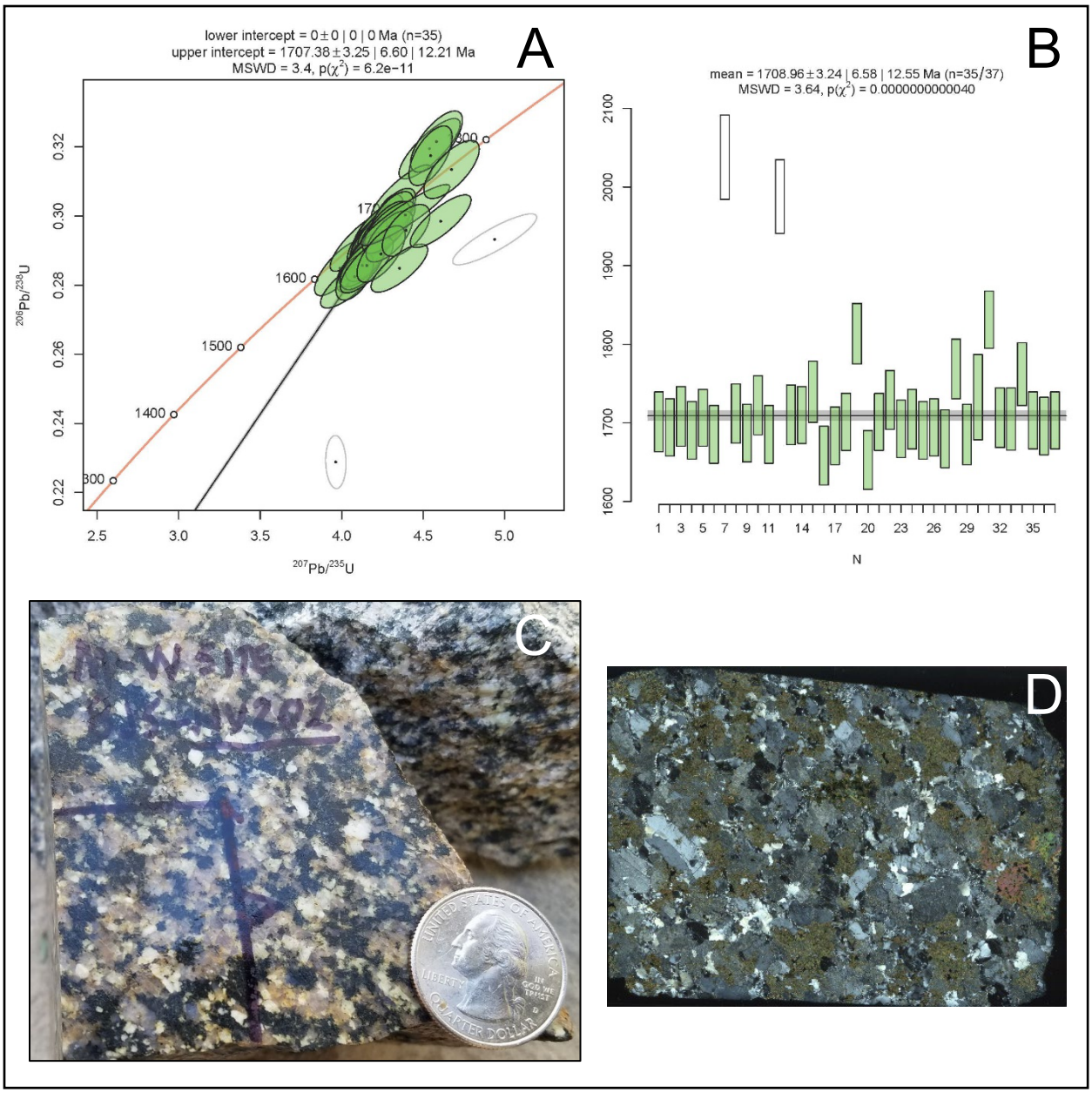

Figure B12. Sample BJS-NV202

Granodiorite of Crippled Jack Well collected near Miller and Wooden Moore Siding sample site (Xcj): (A) Conventional concordia plot with preferred age, (B) mean plot of concordant zircons (C) Sample photograph, (D) Photomicrograph of thin section (crossed polars). Upper intercept age of 1,707 ±7 [35] Ma; MSWD = 3.4, reported based on U-Pb dating of 35 of 37 zircons obtained from the sample. Miller and Wooden (1994) previously reported a U-Pb date of 1659 ±4 Ma on zircon collected at the Moore Siding, based on TIMS analyses.

Luminescence Dating:

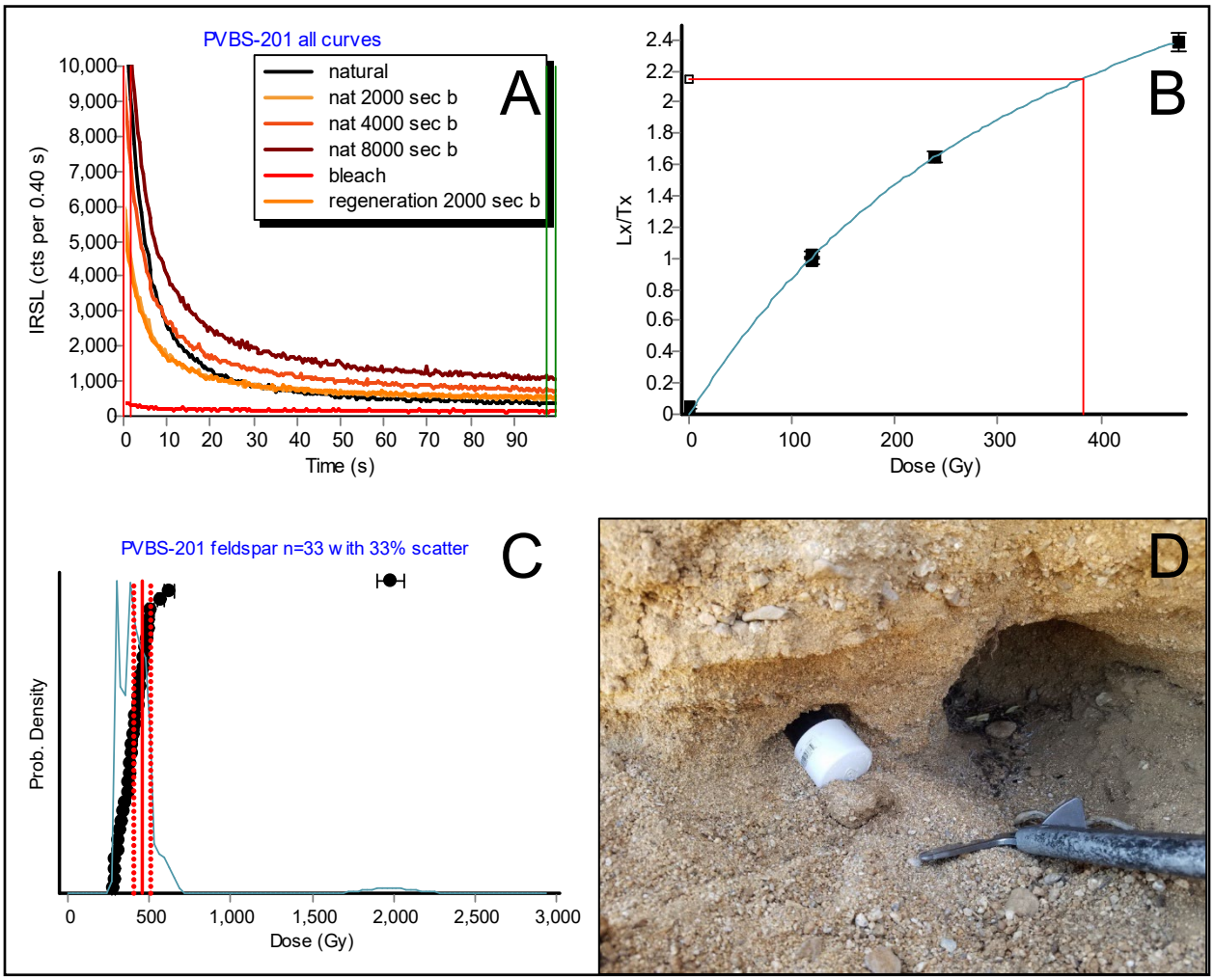

Figure B13. Sample PVBS210

Quaternary older fan deposits sampled along southwest margin of Watson Wash on the east side of New York Mountains. Sample collected about 4 m below original fan surface, which is about 4 m above the adjacent channel grade of Watson Wash: (A) Example of the decay curves for Aliquot #3, (B) Example of the growth curve for Aliquot #3, (C) Probability plot from Riseo Analyst Program, (D) Detail photograph of sample site. Luminescence Central Age Model (CAM) date of 40,740 ±1,450 years based on IRSL dating of 9 aliquots of K-feldspar grains.

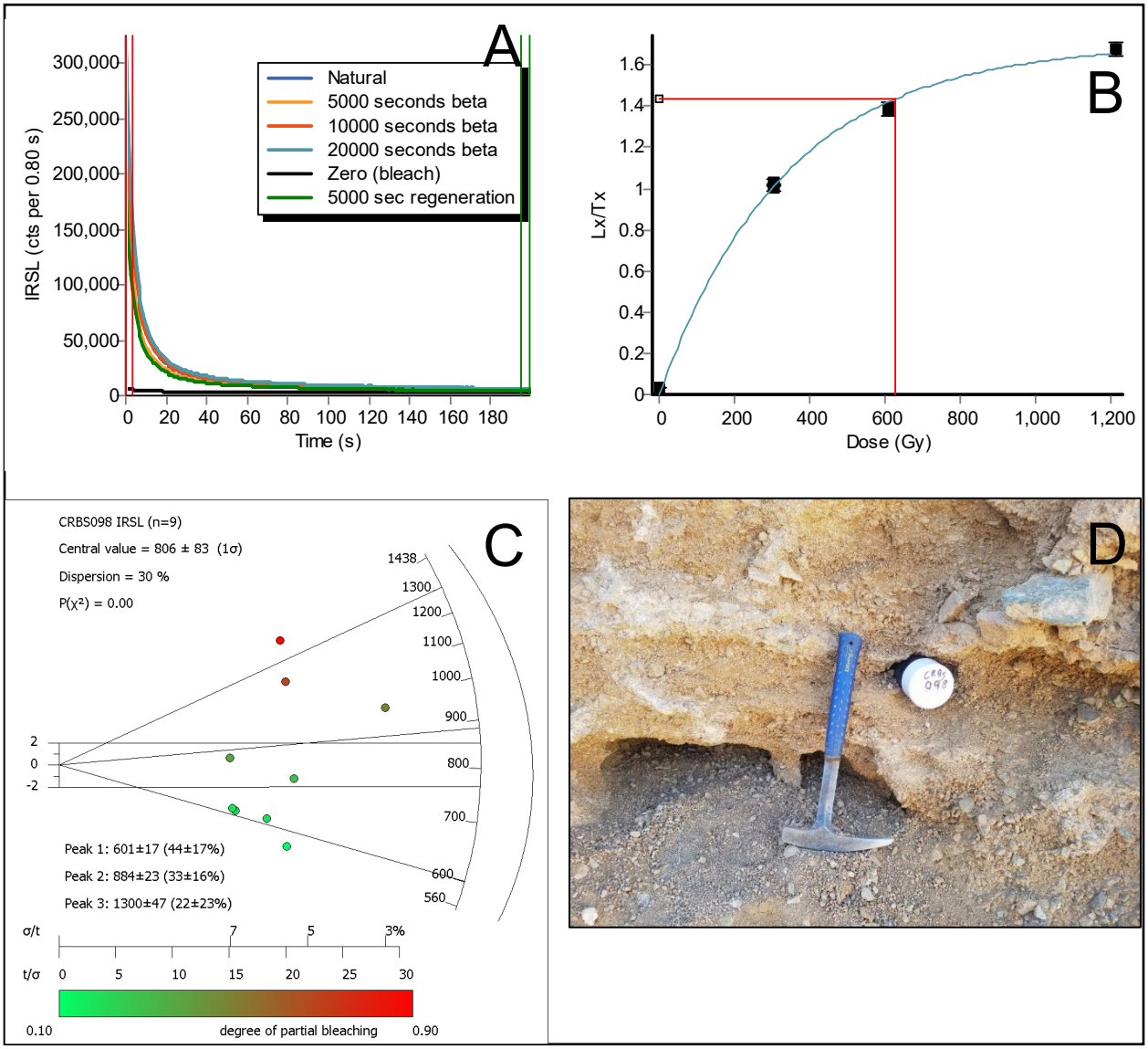

Figure B14. Sample CRBS098

Quaternary older fan deposits sampled on the west side of the New York Mountains. Sample collected about 4 m below original fan surface, which is about 1 m above the adjacent channel grade: (A) Example of the decay curves for Aliquot #10, (B) Example of the growth curve for Aliquot #10, (C) Radial plot of all equivalent dose values (showing population clusters), (D) Detail photograph of sample site. Luminescence Central Age Model (CAM) date of 70,090 ±7,270 years based on IRSL dating of 30 aliquots of K-feldspar grains.

APPENDIX C: GEOCHEMICAL PLOTS

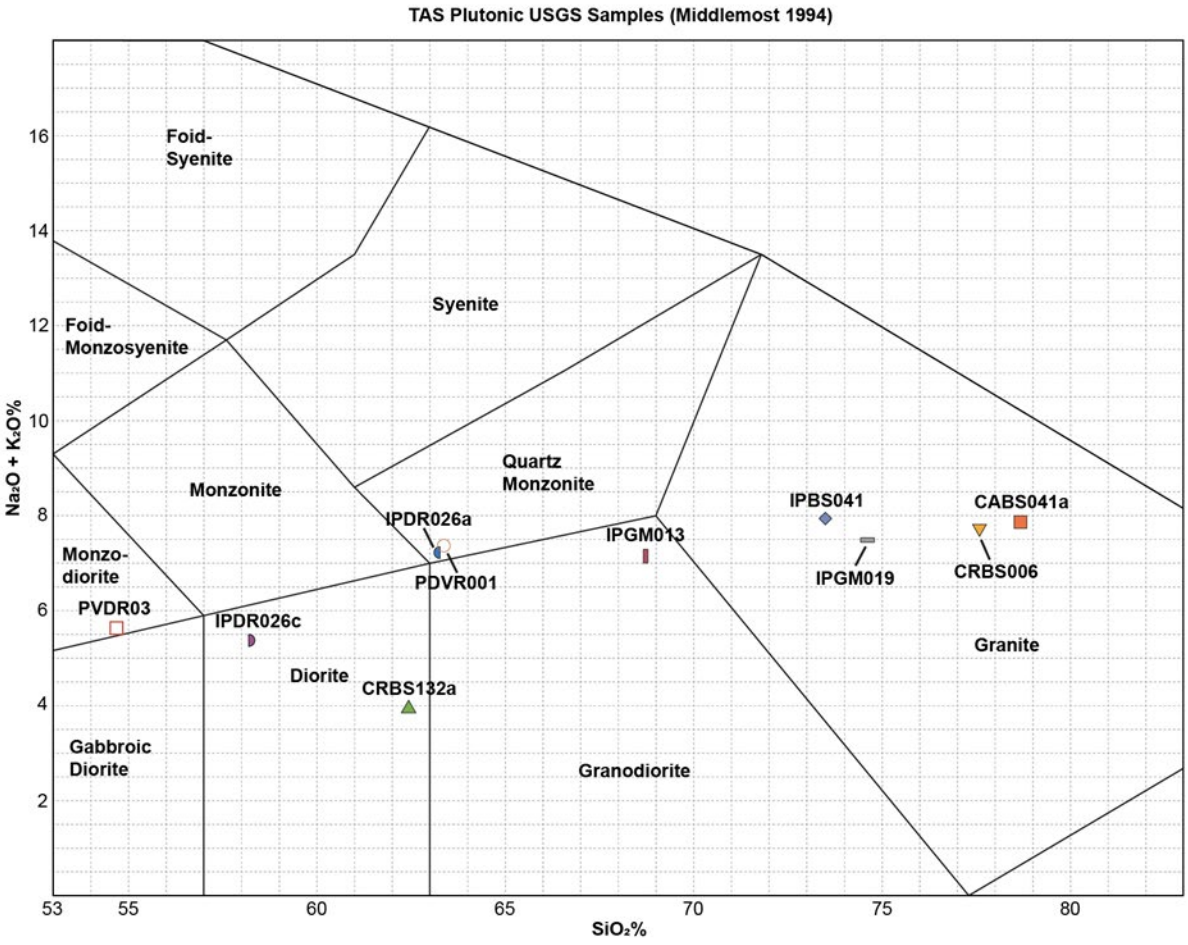

Figure C1. Total Alkali vs. Silica (T.A.S.) classification diagram for USGS geochemistry data
Geochemical samples analyzed by the AGAT Laboratories for USGS. All samples had total oxide weight percent between the range of 98.5-101.5%.

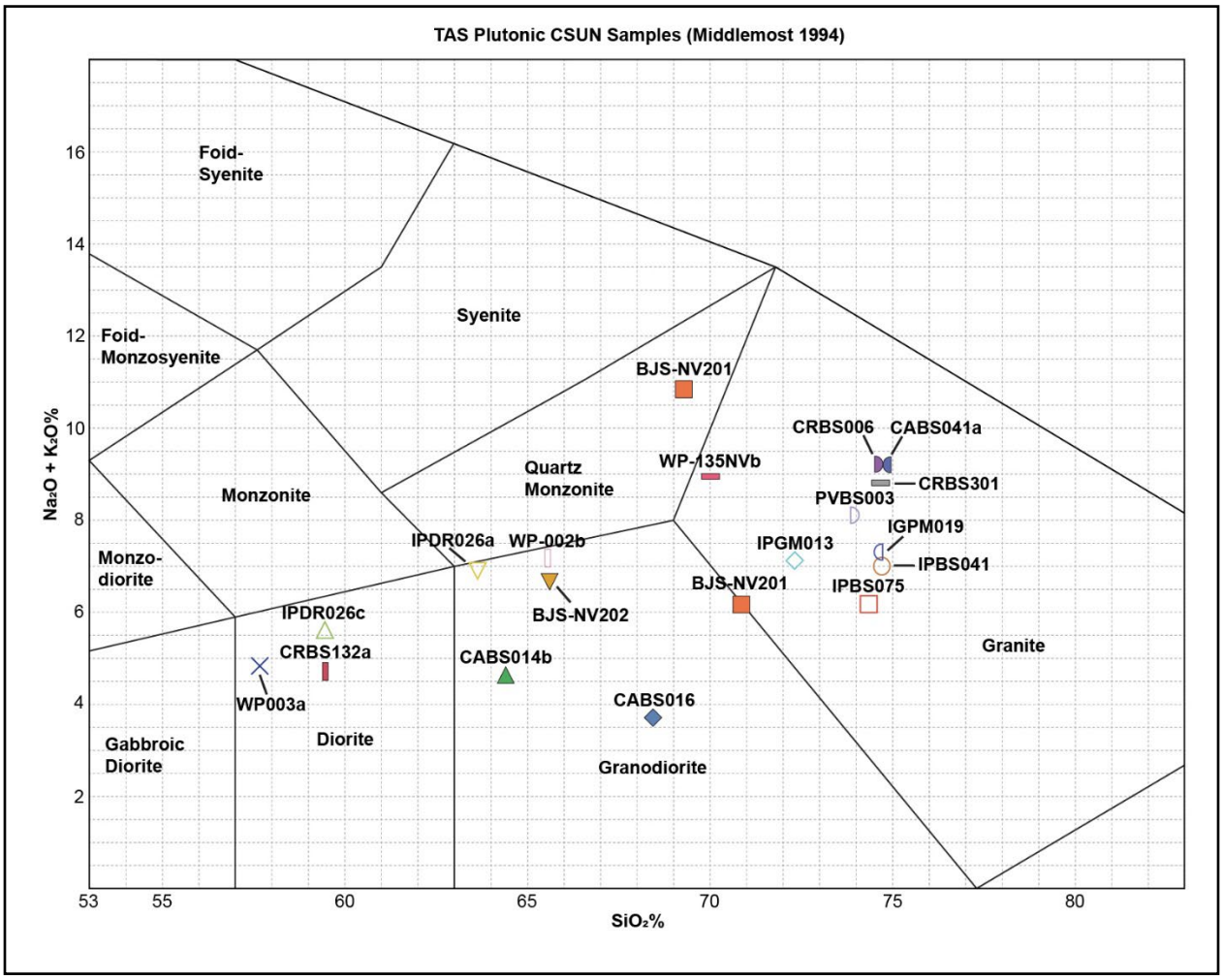

Figure C2. Total Alkali vs. Silica (T.A.S.) classification diagrams for CSUN geochemistry data
Geochemical samples analyzed by Pomona College for CSUN Laser Ablation Laboratory. Sample BJS-NV202 and both IPGM013 and BJS-NV201 samples have total oxide weight above 101.5%.

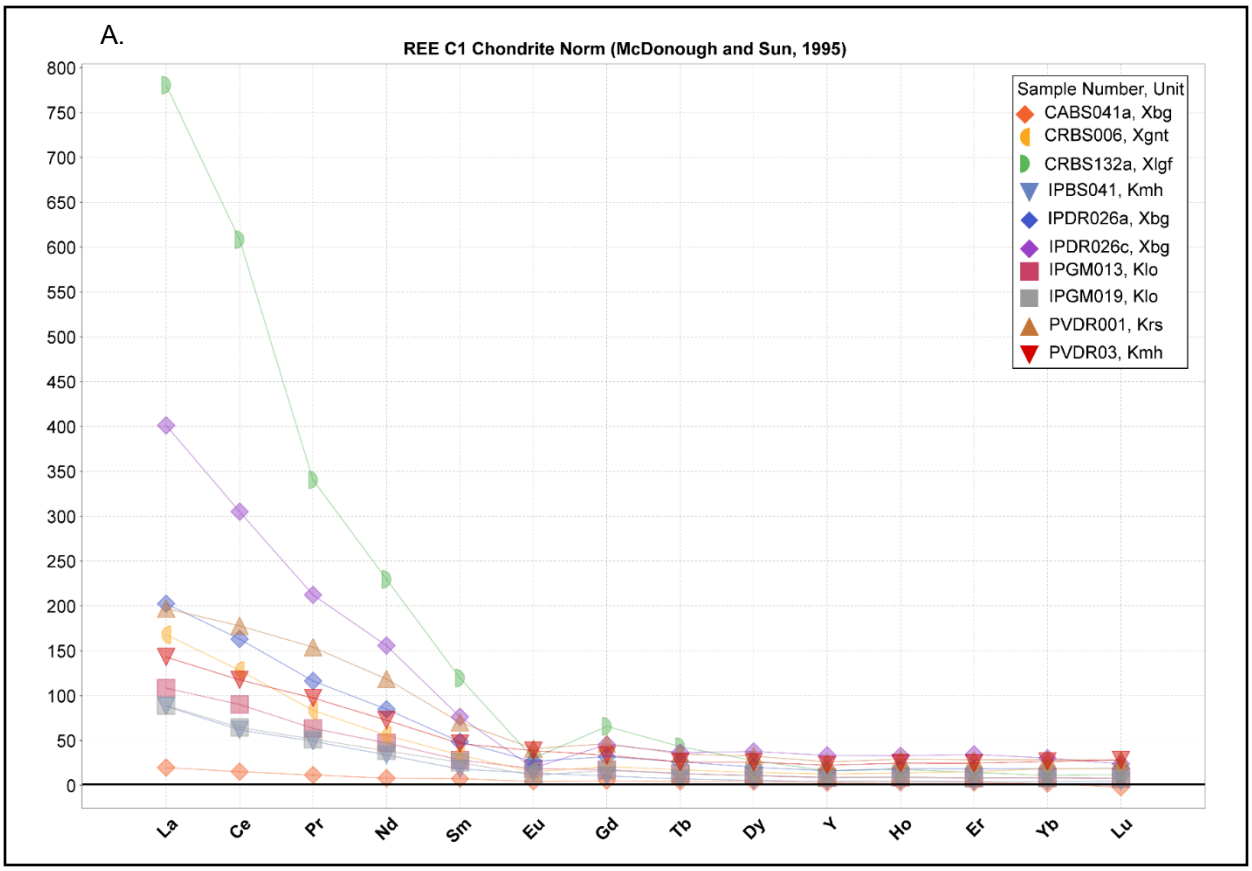

Figure C3. Chondrite-normalized Rare Earth Element (REE) spider diagrams – USGS data

Geochemical samples anayzed by AGAT Laboratories for the USGS plotted on a C1 chondrite standard spinder diagram from Sun and McDonough (1989).

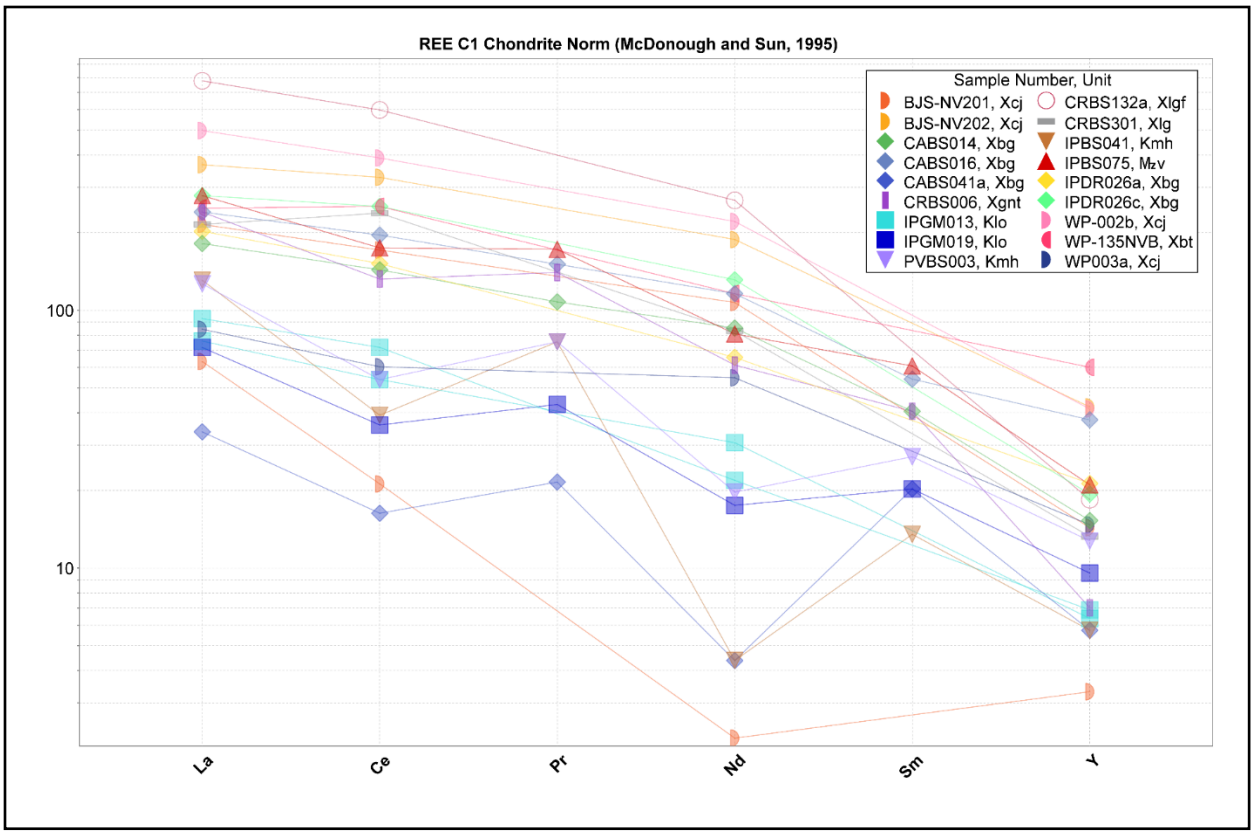

Figure C4. Chondrite-normalized Rare Earth Element (REE) spider diagrams – CSUN data
Geochemical samples anayzed at Pomona College for CSUN Laser Ablation Laboratory, plotted on a C1 chondrite standard spinder diagram from Sun and McDonough (1989).